Mon. Not. R. Astron. Soc. **000**, 1–24 (2010) Printed 22 October 2010 (MN LATEX style file v2.2)

Galaxy stellar mass functions of different morphological types in clusters, and their evolution between z=0.8 and z=0

Benedetta Vulcani[1,2⋆†‡], Bianca M. Poggianti[2], Alfonso Aragón-Salamanca[3], Giovanni Fasano[2], Gregory Rudnick[4], Tiziano Valentinuzzi[1], Alan Dressler[5], Daniela Bettoni[2], Antonio Cava[6,7], Mauro D'Onofrio[1], Jacopo Fritz[8], Alessia Moretti[2], Alessandro Omizzolo[2,9] and Jesús Varela[2]

[1]*Astronomical Department, Padova University, Italy,*
[2]*INAF-Astronomical Observatory of Padova, Italy,*
[3]*School of Physics and Astronomy, University of Nottingham, Nottingham NG7 2RD, UK,*
[4]*Department of Physics and Astronomy, University of Kansas, Lawrence, KS, USA,*
[5]*The Observatories of Carnegie Institution of Washington, Pasadena, CA, USA,*
[6]*Instituto de Astrofisica de Canarias, Spain,*
[7]*Departamento de Astrofisica, Universidad de La Laguna, Spain,*
[8]*Sterrenkundig Observatorium, Vakgroep Fysica en Sterrenkunde, Universiteit Gent, Belgium,*
[9]*Specola Vaticana, Vatican City, Hole See*

Accepted .... Received ..; in original form ...

ABSTRACT

We present the galaxy stellar mass function and its evolution in clusters from $z \sim 0.8$ to the current epoch, based on the WIde-field Nearby Galaxy-cluster Survey (WINGS) ($0.04 \leqslant z \leqslant 0.07$), and the ESO Distant Cluster Survey (EDisCS) ($0.4 \leqslant z \leqslant 0.8$). We investigate the total mass function and find it evolves noticeably with redshift. The shape at $M_* > 10^{11} M_\odot$ does not evolve, but below $M_* \sim 10^{10.8} M_\odot$ the mass function at high redshift is flat, while in the Local Universe it flattens out at lower masses. The population of $M_* = 10^{10.2} - 10^{10.8} M_\odot$ galaxies must have grown significantly between $z = 0.8$ and $z = 0$. We analyze the mass functions of different morphological types (ellipticals, S0s and late-types), and find that also each of them evolves with redshift. All types have proportionally more massive galaxies at high- than at low-z, and the strongest evolution occurs among S0 galaxies. Examining the morphology-mass relation (the way the proportion of galaxies of different morphological types changes with galaxy mass), we find it strongly depends on redshift. At both redshifts, $\sim 40\%$ of the stellar mass is in elliptical galaxies. Another $\sim 43\%$ of the mass is in S0 galaxies in local clusters, while it is in spirals in distant clusters. To explain the observed trends, we discuss the importance of those mechanisms that could shape the mass function. We conclude that mass growth due to star formation plays a crucial role in driving the evolution. It has to be accompanied by infall of galaxies onto clusters, and the mass distribution of infalling galaxies might be different from that of cluster galaxies. However, comparing with high-z field samples, we do not find conclusive evidence for such an environmental mass segregation. Our results suggest that star formation and infall change directly the mass function of late-type galaxies in clusters and, indirectly, that of early-type galaxies through subsequent morphological transformations.

Key words: galaxies: clusters: general — galaxies: evolution — galaxies: formation — galaxies: mass function — galaxies: ellipticals and lenticulars, cD

1 INTRODUCTION

The distribution of galaxy stellar masses at the present day and in the past is of fundamental importance for studying the assembly of galaxies over cosmic time.

It is well known that galaxy properties depend both on galaxy mass and on the environment the galaxies are part of

⋆ E-mail: benedetta.vulcani@oapd.inaf.it;
† visiting The Observatories of Carnegie Institution of Washington, Pasadena, CA, USA
‡ This file has been amended to highlight the proper use of LATEX 2_ε code with the class file. These changes are for illustrative purposes and do not reflect the original paper by B. Vulcani

(e.g. see Baldry et al. 2006; van der Wel 2008; Bolzonella et al. 2009; Tasca et al. 2009). Several studies (e. g. Bundy et al. 2005; Vergani et al. 2008) have shown that mass plays a crucial role in determining galaxy properties and in driving their evolution. Color, specific star formation rate and internal structure are strongly correlated with galaxy stellar mass (Kauffmann et al. 2003). On the other hand, the stellar mass function of galaxies depends on local galaxy density too (e.g. Baldry et al. 2006; Bolzonella et al. 2009), showing that the mass distribution is itself related to environment. In addition, the efficiency of environmental mechanisms can depend on the mass of the galaxy on which they act, and this could cause environmental effects to be interpreted as mass-effects (Tasca et al. 2009).

Clearly, galaxy mass and environment are strictly linked and it is important to analyze them distinctly, trying to separate their relative roles. To disentangle mass and environment it is useful to study the dependence of some properties on mass fixing the environment, or analyze the importance of the environment fixing the mass. In the nature vs nurture scenario, mass represents the primary "intrinsic property" closely related to primordial conditions, while the environment includes all the possible external processes that can influence galaxy evolution.

Stellar mass assembly is usually characterized by the galaxy stellar mass function, that describes the distribution of galaxy masses, at different epochs and different environments. Several studies have been carried out focusing on the importance of the galaxy mass functions in the general field (e.g. Fontana et al. 2006; Drory et al. 2005; Gwyn & Hartwick 2005; Bundy et al. 2006; Pozzetti et al. 2007).

For galaxies with $M \geqslant 10^{11} M_{\odot}$, several studies (eg. Fontana et al. 2004; Bundy et al. 2006; Borch et al. 2006) have found that, overall, the evolution of the total mass function from $z = 1$ to $z = 0$ is relatively modest, which implies that the evolution of objects with mass close to the local characteristic mass is essentially complete by z$\sim$1. However, Fontana et al. (2006) found that less massive galaxies evolve more than massive ones. Moreover, Pozzetti et al. (2009) showed a very fast rise of the total mass function from z$\sim$1 for $M \leqslant 10^{11} M_{\odot}$ and they found this trend is due to star formation driving the mass assembly at intermediate and low masses. Instead, at high masses this process does not play an important role and, as a consequence, Pozzetti et al. (2009) found again that at high masses there is an almost negligible evolution from $z \sim 1$ to $z \sim 0$.

It is interesting to investigate how galaxies of different types give a different contribution to the mass function, shaping, for example, either the massive tail or the low mass tail of the total mass distribution. There are several ways to subdivide galaxies into at least two populations, usually either according to their star formation histories (being passive or star-forming, for example using a rest-frame color, hence separating blue and red galaxies, their SEDs, their spectroscopic features) or their structure (structural parameters or morphologies).

In the Local Universe, a sort of bimodality in galaxy properties has been observed: more massive galaxies tend to be passive, have high surface mass densities, redder colors and have spectra characterized by a pronounced break at $\lambda \sim$4000 Å, while lower-mass galaxies have low surface mass densities, tend to be still star forming, show bluer colors and have spectra characterized by emission lines (Kauffmann et al. 2003; Brinchmann et al. 2004). Baldry et al. (2004), Baldry et al. (2006) and Baldry et al. (2008), subdividing galaxies depending on their colors, found a bimodal shape in the local mass function in the field with an upturn related to the two different populations: early-type galaxies dominate the high masses, while late-types dominate at low/intermediate masses (Pozzetti et al. 2009).

Many studies have been performed to investigate the behavior of this bimodality at higher redshifts: for example, Borch et al. (2006), who subdivide galaxies depending on their color, Fontana et al. (2004), Bundy et al. (2006) and Vergani et al. (2008), who use spectral features to subdivide galaxies with different properties. Although using different techniques, all of them emphasize that the mass functions separately for early-type and late-type galaxies depend on redshift. Early-type galaxies always dominate the massive end, while late-type galaxies mostly contribute to the intermediate/low-mass part of the mass function at all redshifts. From $z \sim 1$ to $z \sim 0$, early-type galaxies show a rapid evolution in their mass function, while late-type galaxies show a relatively little change. This has been interpreted as the result of mass growth due to star formation in late-type galaxies, accompanyed by a subsequent cessation of star formation in some of the blue galaxies, that turn red and contribute to the build-up of the red galaxy population (Bell et al. 2007).

Few studies have attempted to investigate the mass functions of different galaxy types as a function of environment (see e.g. Balogh et al. 2001; Bundy et al. 2006). Bolzonella et al. (2009), classifying galaxies following a spectral energy distribution classification, found that the shape of the mass function of different galaxy types is the same in environments with different local density, so they argued for the existence of a quasi-universal mass function for each type regardless of environment, and also argued for a quasi-universal evolution of the mass function of each type.

The studies mentioned above all focus on the mass functions of galaxies with different stellar histories in the general field, but a clear picture on the stellar mass assembly and how it depends on the mass (mass-assembly downsizing) and galaxy types has not yet emerged.

Fewer studies have focused on the mass functions as a function of galaxy morphology. All of them consider galaxies in the general field. Bundy et al. (2005); Pannella et al. (2006); Franceschini et al. (2006) investigated mass functions of different morphological types, using ACS/HST images to classify galaxies. They found that, at $z \sim 1$, morphologically early- and late-types are present in similar numbers at all masses. By $z \sim 0.3$, ellipticals dominate the high mass population, suggesting that merging or some other transformation process is active. At all redshifts, they found that late-type galaxies dominate at lower masses, while early-type galaxies become prominent at higher masses.

Using both a spectral and a morphological classification, Ilbert et al. (2010) found that most of massive quiescent galaxies have an elliptical morphology at $z <$0.8. They also show similar mass functions. Therefore, a dominant mechanism has to link the shutdown of star formation and the acquisition of an elliptical morphology in massive galaxies.

As the evolution of the mass functions of passive versus star-forming galaxies must be influenced by the quenching of star formation in previously star-forming galaxies (Bell et al. 2007), the evolution in the mass functions of different morphological types must be influenced by the transformation between $z = 1$ and $z = 0$ of some late-type galaxies into early-type galaxies, of which evidence has accumulated both in the field and, especially, in clusters.

In the field, Bundy et al. (2005) found evidence for the transformation of late- into early-type galaxies as a function of time. Based on the observed mass functions, this transformation process appears to be more important at lower masses ($M_{*} \leqslant 10^{11} M_{\odot}$)

because the most massive early-type galaxies are already in place at z∼1. Similarly, Oesch et al. (2010) showed that the evolution of the morphological distribution in galaxies since $z \sim 1$ depends strongly on stellar mass: ellipticals dominate the entire population since z=1, and the Hubble sequence has quantitatively settled down by this epoch. Most of the morphological evolution from z=1 to z=0.2 takes place at masses $M_* \leqslant 10^{11} M_\odot$, where the fraction of spirals substantially drops and the contribution of early-types increases.

Capak et al. (2007) found that in the field galaxies are transformed from late- to early-type galaxies more rapidly in dense than in sparse regions. Comparing their field data to cluster data, they found that in clusters transformations occur even more rapidly.

The morphological evolution is much more striking in clusters, where indeed was discovered: the fraction of late-type galaxies is much higher, and the fraction of S0 galaxies proportionally lower, in distant than in nearby clusters, suggesting an evolution from late to early-type galaxies for a significant fraction of today's early-type galaxies in clusters (Dressler et al. 1997, Fasano et al. 2000, Postman et al. 2005, Smith et al. 2005, Desai et al. 2007). Interestingly, the same studies find that the fraction of ellipticals in clusters does not evolve with redshift.

It isn't surprising that the impact of morphological transformations depends on environment. In clusters, galaxies are expected to be affected by a number of physical processes that can alter the course of their evolution. Galaxies in dense environments are subject to a variety of external stresses, which are, in general, not conductive to the maintenance of spiral structure: i.e. ram pressure (Gunn & Gott 1972; Bekki 2009), galaxy harassment (Moore et al. 1996), cluster tidal forces (Byrd & Valtonen 1990), interaction/merging (Icke 1985; Bekki 1998), strangulation (Larson et al. 1980; Font et al. 2008; McCarthy et al. 2008) can act with different efficiency depending on environment, so field galaxies infalling into larger structures can be transformed from gas-rich spirals to gas-poor lenticular galaxies.

Until now, a few studies of the mass function of galaxies in clusters has been carried out, due to the few observations available. Kodama & Bower (2003) have estimated the stellar mass function for two clusters at $z \sim 1$ transforming their K_s-band luminosity function by correcting it for the star formation contribution as estimated from the J-K_s colours. This and other works (e.g. Aragón-Salamanca et al. 1993; Barger et al. 1998; Toft et al. 2004; Andreon 2006; De Propris et al. 2007) have highlighted the fact that the evolution of the characteristic luminosity $M_\star$ at red wavelengths in clusters is consistent with passive evolution and with massive cluster galaxies being fully assembled by $z \sim 1$. In particular, Toft et al. (2004) pointed out an evolution in the faint end slope of the K_s-band luminosity function of one cluster at $z = 1.2$, suggesting that clusters at $z \sim 1$ contain relatively smaller fractions of low mass galaxies than clusters in the local Universe.

In this context, the WIde-field Nearby Galaxy-cluster Survey (WINGS) (Fasano et al. 2006) and the ESO Distant Cluster Survey (EDisCS) (White et al. 2005), two surveys whose main aims are to characterize clusters and their galaxies at low and high redshift respectively, represent a significant increase in the number of well studied clusters at low and high redshift respectively.

In this paper we focus on the evolution of the galaxy mass functions in clusters. We first analyze the total mass function, and then separately the mass functions of different morphological types and the evolution of the morphological fractions, with the aim of understanding the mechanisms that drive the evolution of the mass distributions.

This paper is organized as follows. In §2 we present the datasets used (WINGS and EDisCS), describing the surveys and the clusters selection at different redshifts; in §3 we derive stellar masses. In §4 we present the mass and magnitude limited galaxy samples, and other galaxy properties we need for the analysis. We then show the total mass function and its evolution with redshift (§5.1), and the mass functions of different galaxy morphological types (§5.2) and their evolution from $z \sim 0.8$ to the current epoch (§5.3). In §6 we analyze the morphology-mass relation, the evolution of the morphological fractions and of the mass fractions in each morphological type. In §7 we comment our findings, discussing the possible mechanisms that are responsible for the observed evolution. Finally, in §8 we summarize our conclusions.

Throughout this paper, we assume $H_0 = 70\,\mathrm{km\,s^{-1}\,Mpc^{-1}}$, $\Omega_m = 0.30$, $\Omega_\Lambda = 0.70$. The adopted initial mass function (IMF) is a Kroupa (2001) in the mass range 0.1-100 $M_\odot$.

2 THE DATA SAMPLES

To perform the study of the mass distribution of galaxies of different morphological types and its evolution from $z \sim 0.8$ to the current epoch, we assemble two galaxy cluster samples in two redshift intervals: the sample at low-z is selected from the WIde-field Nearby Galaxy-cluster Survey (WINGS) (Fasano et al. 2006), while the sample at high-z is selected from the ESO Distant Cluster Survey (EDisCS) (White et al. 2005).

2.1 Low-z sample: WINGS

WINGS[1] (Fasano et al. 2006) is a multiwavelength survey of clusters at $0.04 < z < 0.07$ whose main goal is to characterize the photometric and spectroscopic properties of galaxies in nearby clusters and to describe the changes of these properties depending on galaxy mass and environment.

Clusters were selected in the X-ray from the ROSAT Brightest Cluster Sample and its extension (Ebeling et al. 1998, 2000) and the X-ray Brightest Abell-type Cluster sample (Ebeling et al. 1996). WINGS clusters cover a wide range of velocity dispersion σ_{clus} (typically $500-1100\,km\,s^{-1}$) and a wide range of X-ray luminosity L_X (typically $0.2-5\times10^{44} erg\,s^{-1}$).

The survey is mainly based on optical B, V imaging of 78 galaxy clusters (Varela et al. 2009), that has been complemented by a spectroscopic survey of a subsample of 48 clusters, obtained with the spectrographs WYFFOS@WHT and 2dF@AAT (Cava et al. 2009), by a near-infrared (J, K) survey of a subsample of 28 clusters obtained with WFCAM@UKIRT (Valentinuzzi et al. 2009), and by U broad-band and H_α narrow-band imaging of a subset of WINGS clusters, obtained with wide-field cameras at different telescopes (INT, LBT, Bok) (Omizzolo et al. 2010).

The spectroscopic target selection was based on the WINGS B, V photometry. The aim of the target selection strategy was to maximize the chances of observing galaxies at the cluster redshift without biasing the cluster sample. We selected galaxies with a total $V \leqslant 20$ magnitude and a V magnitude within the fiber aperture of V < 21.5 and with a color within a 5 kpc aperture of $(B-V)_{5kpc} \leqslant 1.4$, to reject background galaxies, much redder than the cluster red sequence. The exact cut in color was varied slightly from cluster to cluster in order to account for the redshift variation and to optimize

[1] http://web.oapd.inaf.it/wings

cluster name	z	σ ($km s^{-1}$)	DM *(mag)*
A1069	0.0653	690± 68	37.34
A119	0.0444	862± 52	36.47
A151	0.0532	760±55	36.87
A1631a	0.0461	640±33	36.55
A1644	0.0467	1080± 54	36.58
A2382	0.0641	888± 54	37.30
A2399	0.0578	712± 41	37.06
A2415	0.0575	696± 51	37.05
A3128	0.06	883± 41	37.15
A3158	0.0593	1086± 48	37.12
A3266	0.0593	1368± 60	36.12
A3376	0.0461	779± 49	36.55
A3395	0.05	790± 42	36.73
A3490	0.0688	694± 52	37.46
A3556	0.0479	558± 37	36.64
A3560	0.0489	710± 41	36.68
A3809	0.0627	563± 40	37.25
A500	0.0678	658±48	37.42
A754	0.0547	1000± 48	36.94
A957x	0.0451	710± 53	36.50
A970	0.0591	764± 47	37.11

Table 1. List of WINGS clusters analyzed in this paper and their redshift *z*, their velocity dispersion σ and their distance modulus *DM*.

the observational setup. These very loose selection limits were applied so as to avoid any bias in the colors of selected galaxies.

In this paper, we only consider spectroscopically confirmed members of 21 of the 48 clusters with spectroscopy. This is the subset of clusters that have a spectroscopic completeness (the ratio of the number of spectra yielding a redshift to the total number of galaxies in the photometric catalog) larger than 50%. The completeness is determined using V-band magnitudes and turns out to be rather flat with magnitude for most clusters, for the reasons discussed in Cava et al. (2009). Moreover, completeness is essentially independent from the distance to the centre of the cluster for most clusters.

Our imaging covers a $34' \times 34'$ field, that corresponds to about 0.6 R_{200}, for all the 21 clusters considered, except for *A1644* and *A3266* where the $\sim 0.5 R_{200}$ is covered. R_{200} is defined as the radius delimiting a sphere with interior mean density 200 times the critical density of the Universe at that redshift, and is commonly used as an approximation for the cluster virial radius. The R_{200} values for our structures are computed from the velocity dispersions by Cava et al. (2009).

Galaxies are considered members of a cluster if their spectroscopic redshift lies within $\pm 3\sigma$ from the cluster mean redshift, where σ is the cluster velocity dispersion (Cava et al. 2009).

The clusters used in this analysis are listed in Table 1.

2.2 High-z sample: EDisCS

EDisCS is a multiwavelength photometric and spectroscopic survey of galaxies in 20 fields containing galaxy clusters at $0.4 < z < 1$ (White et al. 2005). Its main goal is to characterize both the clusters themselves and the galaxies within them.

Clusters were drawn from the Las Campanas Distant Cluster Survey (LCDCS) catalog (Gonzalez et al. 2001). They were selected as surface brightness peaks in smoothed images taken with a very wide optical filter ($\sim 4500-7500$ Å). The redshifts of the LCDCS cluster candidates were initially estimated from the apparent magnitude of the brightest cluster galaxy (BCG). The 20 EDisCS fields were chosen among the 30 highest surface brightness candidates, after confirmation of the presence of an apparent cluster and of a possible red sequence with VLT 20 min exposures in two filters (White et al. 2005). Then, all candidates were subdivided in two groups, the first one at intermediate redshift ($z \sim 0.5$) and the second one at high redshift ($z \sim 0.8$).

For all 20 fields, EDisCS has obtained deep optical multiband photometry with FORS2/VLT (White et al. 2005) and near-IR photometry with SOFI/NTT (Aragón-Salamanca et al. 2010). Photometric redshifts were measured using both optical and infrared imaging (Pelló et al. 2009). Their determinations, their performance, and their use to isolate cluster members, are described in detail in Pelló et al. (2009) and Rudnick et al. (2009), and are briefly summarized in the following. Photometric redshifts were computed for every object in the EDisCS fields using two independent codes, a modified version of the publicly available Hyperz code (Bolzonella et al. 2000) and the code of Rudnick et al. (2001) with the modifications presented in Rudnick et al. (2003). The accuracy of both methods is $\sigma(\delta z) \sim 0.05-0.06$, where $\delta z = \frac{zspec-zphot}{1+zspec}$. Membership was established using a modified version of the technique first developed in Brunner & Lubin (2000), in which the probability of a galaxy to be at redshift z ($P(z)$) is integrated in a slice around the cluster redshift to give P_{clust} for the two codes. The width of the slice around which $P(z)$ is integrated should be of the order of the uncertainty in redshift for the galaxies in question. In our case a $\Delta z = \pm 0.1$ slice around the spectroscopic redshift of the cluster z_{clust} was used. A galaxy was rejected from the membership list if P_{clust} was smaller than a certain probability P_{thresh} for either code. The P_{thresh} value for each cluster was calibrated from our spectroscopic redshifts and was chosen to maximize the efficiency with which we can reject spectroscopic non-members while retaining at least $\sim 90\%$ of the confirmed cluster members, independent of their rest-frame (B-V) color or observed (V-I) color. In practice we were able to choose thresholds such that we satisfied this criterion while rejecting 45%-70% of spectroscopically confirmed non-members. Applied to the entire magnitude limited sample, our thresholds reject 75%-93% of all galaxies with $I_{tot} < 24.9$. A posteriori, we verified that in our sample of galaxies with spectroscopic redshift and above the mass limit described below, $\sim$20% of those galaxies that are photo-z cluster members are spectroscopically interlopers and, conversely, only $\sim$6% of those galaxies that are spectroscopic cluster members are rejected by the photo-z technique.

Deep spectroscopy with FORS2/VLT was obtained for 18 of the fields (Halliday et al. 2004; Milvang-Jensen et al. 2008). Spectroscopic targets were selected with the aim to produce an unbiased sample of cluster galaxies. Conservative rejection criteria based on photometric redshifts (different from those adopted to assess the photo-z membership described above) were used in the selection of spectroscopic targets to reject a significant fraction of non-members, while retaining an unbiased spectroscopic sample equivalent to a purely I-band selected one. Typically, spectra of more than 100 galaxies per field were obtained, with I$\leqslant$22 for the z$\sim$0.5 cluster candidates and I$\leqslant$23 for the z$\sim$ 0.8 ones.

ACS/HST mosaic imaging in $F814W$ of 10 of the highest redshift clusters has also been acquired (Desai et al. 2007), covering with four ACS pointings a $6.5' \times 6.5'$ field with an additional deep pointing in the centre. This field covers the R_{200} of all clusters, except for *cl 1232.5-1250* (Poggianti et al. 2006). The R_{200} values

cluster name	z	σ ($km\,s^{-1}$)
cl 1040.7-1155	0.70	418^{+55}_{-46}
cl 1054.4-1146	0.70	589^{+78}_{-70}
cl 1054.7-1245	0.75	504^{+113}_{-65}
cl 1103.7-1245	0.62	336^{+36}_{-40}
cl 1138.2-1133	0.48	732^{+72}_{-76}
cl 1216.8-1201	0.79	1018^{+73}_{-77}
cl 1227.9-1138	0.64	574^{+72}_{-75}
cl 1232.5-1250	0.54	1080^{+119}_{-89}
cl 1354.2-1230	0.76	648^{+105}_{-110}

Table 2. List of EDisCS clusters analyzed in this paper, with cluster name, redshift z and velocity dispersion σ (from Halliday et al. 2004; Milvang-Jensen et al. 2008).

for our structures are computed from the velocity dispersions by Poggianti et al. (2008).

In this paper, to have a large sample of galaxies at high redshift (see below), we analyze the data of photo-z members of 9 EDisCS clusters, for which *HST* images and, consequently, morphologies were available. Even though *HST* data for *cl 1037.7-1243* are available, this cluster has no galaxies above the completeness limits we will adopt, hence in our analysis we do not consider it. Table 2 presents the list of clusters used.

3 GALAXY STELLAR MASSES ESTIMATES

In this paper we adopt the Kroupa (2001) IMF in the mass range 0.1-100 $M_{\odot}$ to compute the galaxy stellar masses. We determine them in the same way for both data-sets. We follow Bell & de Jong (2001) who used a spectrophotometric model finding a strong correlation between stellar mass-to-light (M/L) ratio and opticals colors of the integrated stellar populations for a wide range of star formation histories. They found that this correlation is quite robust to uncertainties in stellar population and galaxy evolution models.

We determine stellar masses using the relation between M/L_B and rest-frame $(B-V)$ color and the equation given in Bell & de Jong (2001):

$$\log_{10}(M/L_B) = a_B + b_B(B-V) \quad (1)$$

For the Bruzual & Charlot model with a Salpeter (1955) IMF (0.1-125 $M_{\odot}$) and solar metallicity, a_B = –0.51 and b_B = 1.45. Then, we scale our masses to a Kroupa (2001) IMF adding -0.19 dex to the logarithmic value of the masses.

The choice of the photometric bands is dictated by the fact that we have only B and V for all the WINGS clusters used, and also that the rest-frame B-band has been directly observed for all EDisCS clusters. K-band luminosity would be preferable to determine masses, as the K-band is less sensitive to recent star formation and dust. However, K-band is available only for a subset of the WINGS clusters considered, and K-band wavelengths have not been directly observed by EDisCS, for which K-band magnitudes were extrapolated from the photo-z templates.

3.1 Low-z: WINGS

For WINGS spectroscopically confirmed cluster galaxies, the total luminosity L_B has been derived from the total (Sextractor AUTO) observed B magnitude (Varela et al. 2009), corrected for distance modulus and foreground Galaxy extinction, and k-corrected using tabulated values from Poggianti (1997). The B-V color used to calculate masses was derived from observed B and V aperture magnitudes measured within a diameter of 10 kpc around each galaxy baricenter, corrected as the total magnitude.

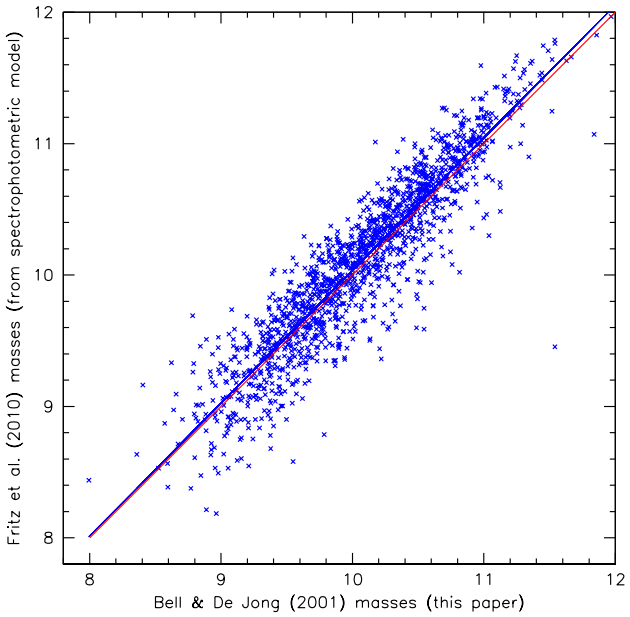

Figure 1. Comparison between the determination of WINGS masses used in this paper and those derived from the spectrophotometric model (Fritz et al. 2007, 2010). All masses are converted to a Kroupa (2001) IMF in the mass range 0.1-100 $M_{\odot}$. Points are logarithmic values. The blue line is the best fit to the points, and the red line is the 1:1 relation.

Stellar masses for WINGS galaxies had been previously determined by fitting the optical spectrum (in the range $\sim$ 3600– $\sim$ 7000 Å) (Fritz et al. 2010), with the spectro-photometric model fully described in Fritz et al. (2007). In this model, all the main spectrophotometric features are reproduced by summing the theoretical spectra of Simple Stellar Population (SSP) of 13 different ages (from 3×10^6 to $\sim 14\times10^9$ years). Dust extinction is allowed to vary as a function of SSP age, and the metallicity can vary among three values: Z=0.004, Z=0.02 and Z=0.05. These mass estimates were then corrected for color gradients within each galaxy (i.e. for the difference in color within the fibre and over a 10kpc diameter). For a detailed description of the determination of masses see Valentinuzzi et al. (2010) and Fritz et al. (2010).

The comparison of masses used in this paper with masses determined by the Fritz et al. (2010) spectro-photometric model converted to the adopted IMF (see Fig. 1) shows no offset between the two estimates, and an rms of $\sim$ 0.3 dex that we adopt as the typical error on the masses. Above $\log M_*/M_{\odot}$ = 9.8, that is the WINGS mass completeness limit (see §4.1.1) there is an offset of $\sim$ 0.06 dex and the rms is $\sim$ 0.3 dex. An exhaustive comparison among masses and errors determined from different bands can be found in Fritz et al. (2010).

For homogeneity with the EDisCS mass estimates (see next section), throughout this paper we only use Bell & de Jong (2001) masses.

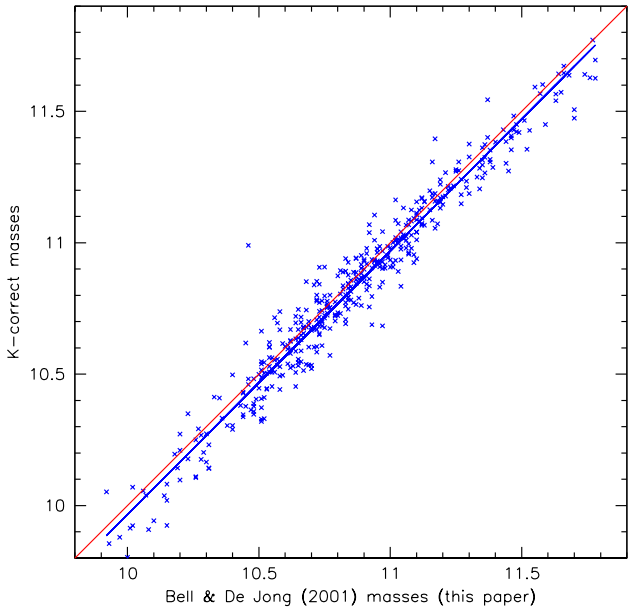

Figure 2. Comparison between the determination of EDisCS masses used in this paper and those derived using the *k-correct* tool (Blanton & Roweis 2007). Only galaxies for which spectroscopy is available are considered. All masses are converted to a Kroupa (2001) IMF in the mass range 0.1-100 $M_{\odot}$. Points are logarithmic values. The blue line is the best fit to the points, and the red line is the 1:1 relation.

3.2 High-z: EDisCS

For EDisCS galaxies, stellar masses for spectroscopic members were estimated by John Moustakas (2009, private communication) using the *kcorrect* tool (Blanton & Roweis 2007)[2], that models the available observed broad band photometry, fitting templates obtained with spectrophotometric models.

For this paper, to be fully consistent with stellar masses of the sample at low-z, we have estimated stellar masses following again the method proposed by Bell & de Jong (2001), using total absolute magnitudes derived from photo-z fitting fixing each galaxy redshift to be equal to the spectroscopic redshift of the cluster it belongs to (Rudnick et al. 2003; Pelló et al. 2009), converting our values to a Kroupa (2001) IMF.

In Figure 2, a comparison of the two methods is shown only for spectroscopic members of all EDisCS clusters (not just the 9 with HST used in this paper). There is a satisfactory agreement, with a systematic offset of 0.03 dex and an rms of 0.08 dex. If we consider data only above the EDisCS completeness limit ($\log M_*/M_{\odot} \geqslant 10.4$, see §4.2.1), we find a mean offset of ~ 0.09 dex and an rms of 0.08 dex.

Finally, we note that a only slightly larger systematic offset and rms (0.13 and 0.13, respectively) are found when comparing the masses of EDisCS spectroscopic members derived with the Bell & de Jong (2001) method with those derived by fitting the EDisCS spectra using the non-parametric method of Ocvirk et al. (2006); Ocvirk (2010), the new models of Vazdekis (2009) and the MILES stellar library of Sánchez-Blázquez et al. (2006).

[2] http://cosmo.nyu.edu/mb144/kcorrect/

4 GALAXY SAMPLES

Both at high- and low-z, we analyze the mass functions and the fractions of galaxies of different morphological types, as determined by high-quality imaging. For this purpose, galaxies are divided in three groups: ellipticals, lenticulars (or S0s) and late-type galaxies (spirals + irregulars). In some cases, we will also consider ellipticals and S0s together, defined as early-type galaxies.

In the following, depending on our aim, we use two different methods of galaxy sample selection.

To study the mass distribution of different morphological types (§5), the best is to use a mass limited sample. In this case, the mass limit endorsed needs to be such to ensure completeness, i.e. to include all galaxies more massive than the limit regardless of their color or morphological type. To determine this limit, we compute the mass of an object whose observed magnitude is equal to the faint magnitude limit of the survey, and whose color is the reddest color of a galaxy at the highest redshift considered.

In the subsequent part of the paper (§6), we compare the evolution of the mass distributions with the evolution of the morphological fractions. Since in the literature the latter are available only for a magnitude limited sample, we assemble also galaxy magnitude limited samples. In this case, the minimum detected stellar mass depends both on redshift and galaxy color.

4.1 Low-z sample: WINGS

For WINGS, we consider only spectroscopically confirmed members of our clusters. Using all galaxies in the photometric sample would provide a larger dataset, however for WINGS the photometric data cannot be used to assess cluster membership due to the low redshift and restricted photometric coverage.

Since galaxies with available spectroscopy are only a fraction ($> 50\%$ in the clusters used) of the total number of possible spectroscopic targets, we need to apply a statistical correction to correct for incompleteness. This is obtained weighting each galaxy by the inverse of the ratio of the number of spectra yielding a redshift to the total number of galaxies in the photometric catalog, in bins of 1 mag (Cava et al. 2009).

As in several other works (see e.g. von der Linden et al. 2010), in each cluster, we exclude the BCG, defined as the most luminous galaxy of each cluster, that could alter the mass distribution of the whole sample. In fact, the properties of BCGs are in many respect peculiar with respect to other galaxies, and they are the subject of many separate studies dedicated only to this class of objects. For example, Fasano et al. (2010) found that also in the WINGS dataset BCGs are heterogeneus with respect to the global population of ellipticals for their distribution of apparent (and intrinsic) flattenings.

Only galaxies lying within $0.6R_{200}$ are considered, because this is the largest radius covered approximately in all clusters.

Morphological types are derived from V-band images using MORPHOT, an automatic tool for galaxy morphology, purposely devised in the framework of the WINGS project. MORPHOT was designed with the aim to reproduce as closely as possible visual morphological classifications.

MORPHOT extends the classical CAS (Concentration/Asymmetry/clumpinesS) parameter set (Conselice 2003), by using 20 image-based morphological diagnostics. Fourteen of them have never been used, while the remaining six [besides the CAS parameters, the Sersic index, the Gini and M20 coefficients (Lotz et al. 2004)] are actually already present in the literature, although in slightly different forms. Defining the newly introduced

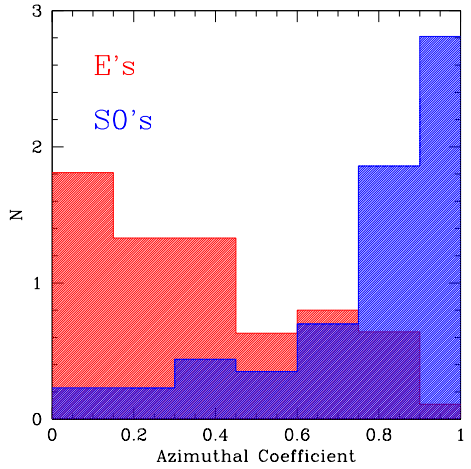

Figure 3. Normalized distributions of the MORPHOT Azimuthal Coefficient for the visually classified ellipticals (366 objects, red histogram) and S0 galaxies (267 objects, blue histogram) of the MORPHOT calibration sample.

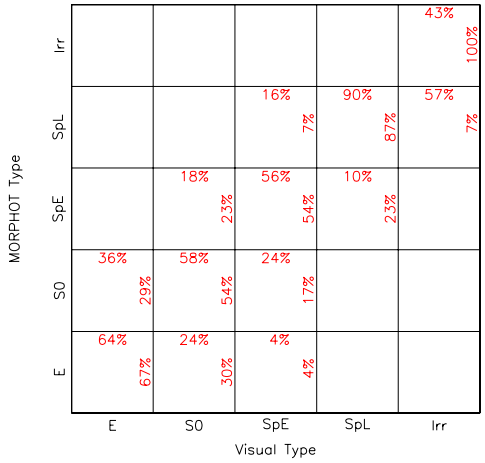

Figure 4. Comparison between visual and MORPHOT broad morphological types for the 931 galaxies of the MORPHOT calibration sample. In the 2D bins of the plot the percentages of visual/MORPHOT broad types in different MORPHOT/visual types are reported in the top/right sides of the bins.

diagnostics and explaining their meaning is beyond the scope of the present paper. We refer the reader to Fasano et al. (2010, Appendix A therein) for an outlining of the logical sequence and the basic procedures of MORPHOT, while an exhaustive description of the tool will be given in a forthcoming paper (Fasano et al., in preparation). Here we just mention that, among the 14 newly devised diagnostics, the most effective one in order to disentangle ellipticals from S0 galaxies turned out to be an Azimuthal coefficient, measuring the correlation between azimuth and pixel flux relative to the average flux value of the elliptical isophote passing through the pixel itself. Figure 3 illustrates the distributions of the Azimuthal coefficient for the samples of ellipticals and S0 galaxies used to calibrate MORPHOT.

More importantly for our purposes, the quantitative discrepancy between automatic (MORPHOT) and visual classifications turns out to be similar to the typical discrepancy among visual classifications given by experienced, independent human classifiers (r.m.s.$\sim$1.5-2.5 T types). This was extensively tested on a calibration sample of 931 WINGS galaxies with both visual and MORPHOT classification, where the visual classification was carried out independently by GF and AD. This is illustrated in Figure 4, where the automatic classification is also shown to be bias-free in the overall range of morphological types.

For now, we can apply MORPHOT just to the WINGS imaging, because the tool is calibrated on the WINGS imaging characteristics, and we defer to a later time a more generally usable version of the tool. To verify directly that the two methods adopted at different redshifts (see Section 4.2) are consistent, we can apply the same "method" (visual classification and persons) that was used at high-z on the low-z images.

To this aim, 3 of the classifiers that in 2007 visually classified all the EDisCS galaxies (BMP, AAS, VD) now performed a visual classification of WINGS galaxies. This was done on the subset of WINGS galaxies that was used to calibrate MORPHOT on the visual WINGS morphologies, including only galaxies that enter the sample we analyze in this paper (173 galaxies).

The results (see Fig.5) show agreement between the three broad morphological classes assigned by the EDisCS classifiers with the WINGS visual classification in $\sim$83% of the cases, and with MORPHOT in $\sim$75% of the cases.

Again, these discrepancies turn out to be similar to the typical discrepancy among visual classifications given by experienced, independent human classifiers, so we conclude that the different methods adopted provide a comparable classification.

4.1.1 *Mass limited sample*

The spectroscopic magnitude limit of the WINGS survey is V=20. Considering the distance module of $\sim$ 37.5 of the most distant WINGS cluster, and a reddest color of $(B-V)$ = 1.2, the magnitude limit corresponds to a mass limit $M_* = 10^{9.8} M_\odot$, above which the sample is unbiased. Adopting this limit, the final sample composed by galaxy cluster members, within $0.6R_{200}$, excluded the BCGs, consists of 1233 galaxies, of which 396 ellipticals galaxies, 586 S0s, 239 late type galaxies and 12 galaxies with no classification (see Table 3). The corresponding numbers weighted for completeness are also given in Table 3, for a total of 1894.42 galaxies. Numbers of WINGS galaxies above the EDisCS mass limit ($M_* = 10^{10.2} M_\odot$, see below) are also listed in Table 3.

4.1.2 *Magnitude limited sample*

Since we will use the morphological fractions derived by Poggianti et al. (2009), we use the magnitude limit adopted in that study, which is M_V=-19.5, corresponding to the passively evolving limit of the EDisCS morphological study at higher redshifts (Desai et al. 2007). The final sample of members within $0.6R_{200}$, excluded the BCGs, consists of 263 ellipticals, 410 S0s, 191 late-type galaxies, and 10 galaxies with no morphological classification, for a total of 874 galaxies, as listed in Table 3. Numbers weighted for completeness, for a total of 1340.73 galaxies, can be found in Table 3.

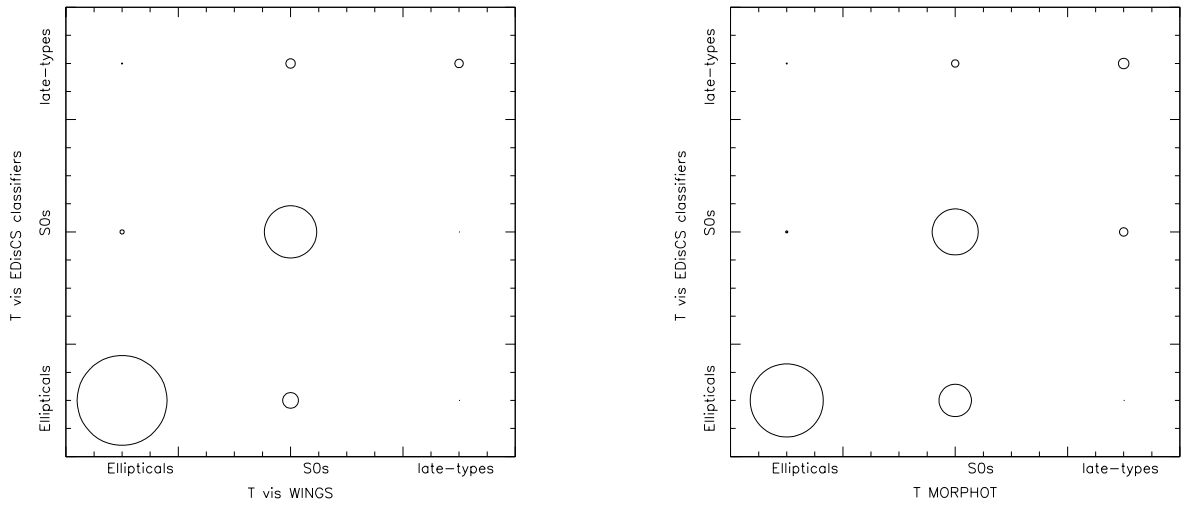

Figure 5. Comparison between the visual classification performed by the EDisCS classifiers and the WINGS visual classification (left panel) and the automatic classification performed by MORPHOT (right panel). The circle radius is proportional to the number of galaxies.

4.2 High-z sample: EDisCS

For EDisCS, there are 605 spectroscopically confirmed members. 381 of them ($\sim$ 63%) have HST morphologies. The spectroscopic magnitude limit ranges between I=22 and I=23 depending on redshift, and the most conservative spectroscopic mass limit using a Kroupa (2001) IMF becomes $M = 10^{10.6} M_{\odot}$ (Vulcani et al. 2010). Therefore, relying only on spectroscopy, the lower mass limit of our study would be very high, and numbers would be relatively small.

For this reason, we decided to use all photo-z members (see §2.2). All the EDisCS mass functions analyzed below are based solely on the photo-z membership, unless otherwise stated. The photo-z technique allows us to push the mass limit to much lower values than the spectroscopy (see below). As shown in Appendix A, spectroscopic and photo-z techniques give very consistent results in the mass range in common.

As for the WINGS sample, BCGs and galaxies at radii greater than $r = 0.6 R_{200}$ have been excluded from the analysis.

Morphologies are discussed in detail in Desai et al. (2007). The morphological classification of galaxies is based on the visual classification of *HST/ACS* F814W images sampling the rest-frame $\sim 4300-5500$ Å range, similarly to WINGS.

4.2.1 *Mass limited sample*

The magnitude completeness limit of the EDisCS photometry is $I \sim 24$, though the completeness clearly remains high to magnitudes significantly fainter than $I = 24$ (White et al. 2005).

We consider the most distant cluster, *cl 1216.8-1201*, that is located at $z \sim 0.8$ and determine the value of the mass of a galaxy with an absolute B magnitude corresponding to $I = 24$, and a color $(B-V) \sim 0.9$, which is the reddest color of galaxies in this cluster. In this way, the EDisCS mass completeness limit based on photo-z is $M_* = 10^{10.2} M_{\odot}$.[3]

The completeness is confirmed by the analysis of Rudnick et al. (2009), who find that for the magnitudes used in this paper (M_g always $\leqslant -20.2$) the photo-z counts are fully consistent with the statistically background subtracted counts for both red and blue galaxies.

The final mass-limited EDisCS sample above this limit consists of 489 galaxies, 156 of which are classified as ellipticals, 64 as S0s, 252 as late-type galaxies, and 17 galaxies with unknown morphology (see Table 3).

4.2.2 *Magnitude limited sample*

We use the same magnitude limit as in the EDisCS morphological study (Desai et al. 2007), M_V=-20, which for passive evolution corresponds to the magnitude limit in the WINGS morphological study (Poggianti et al. 2009). With this limit, our sample consists of 544 galaxies, 151 of which are ellipticals, 67 S0s, 304 late-types, and 22 galaxies with unknown morphologies (see Table 3).

5 RESULTS: THE MASS FUNCTION

In this section we analyze only the mass limited samples of both data-sets.[4]

We use galaxy stellar masses to characterize the mass distribution of different galaxy types in clusters, both at low- and high-z.

Above the completeness limit, we build histograms to define the mass distribution. In each mass bin, we sum all galaxies of all clusters to obtain the total number of galaxies, then we divide this number for the width of the bin, to have the number of galaxies per unit of mass. The width of each mass bin is 0.1 dex. In the case of spectroscopic data, as for WINGS, in building histograms each

[3] Note that with this selection only a few (1.7%) galaxies in the mass-limited sample are fainter than I=23, and therefore have no morphological classification from Desai et al. 2007.

[4] Appendix B presents the mass functions for magnitude limited samples of WINGS and EDisCS galaxies, and clearly shows the biases inherent in this type of selection.

	WINGS						EDisCS	
	$M_* \geqslant 10^{9.8} M_\odot$		$M_* \geqslant 10^{10.2} M_\odot$		$M_V \leqslant -19.5$		$M_* \geqslant 10^{10.2} M_\odot$	$M_V \leqslant -20$
	N_{obs}	N_w	N_{obs}	N_w	N_{obs}	N_w	N	N
all	1233	1894.42	737	1132.55	874	1340.73	489	544
ellipticals	396	603.31	243	367.12	263	397.33	156	151
S0s	586	912.45	369	578.13	410	641.11	64	67
late-types	239	358.52	119	176.84	191	286.13	252	304
unknown	12	20.14	6	10.46	10	16.16	17	22

Table 3. Number of galaxies above the different limits. For WINGS both observed numbers and numbers weighted for spectroscopic incompleteness are given

galaxy is weighted by its incompleteness correction. Errorbars are computed using poissonian errors (Gehrels 1986).

Clusters of different masses could have a different role in the total mass function, so we have tried to test the importance of this effect. For WINGS galaxies, we have determined the mass functions separately for clusters with $\sigma < 700\ km s^{-1}$, $700\ km s^{-1} < \sigma < 800\ km s^{-1}$ and $\sigma > 800\ km s^{-1}$ (plots not shown) and we found no differences. Similarly, for EDisCS galaxies we have tried building the total mass function normalizing for the number of galaxies in each cluster, to avoid the possible larger contribution of larger clusters to the total mass function. Once again, we have found (plots not shown) no differences with the mass function presented in this paper. So, a different combination of the mass functions of different clusters could only influence the final normalization; anyway, since we are interested mainly in the shape of the mass distributions and not in the counts (see below), this doesn't affect our results. Consequently, we conclude that the mass of the cluster, over the cluster mass ranges considered here, does not influence significantly the shape of the total mass function, and in the following we use the simple sum of all galaxies in all clusters.

To quantify the differences between different mass functions, we perform Kolmogorov-Smirnov (K-S) tests. However, the standard K-S test does not consider the completeness issues when it builds the cumulative distribution (since it assigns to each object a weight equal to 1). So we modified the test, to make the relative importance of each galaxy in the cumulative distribution depend on its weight. In the following, we will always use this modified K-S test. Obviously, for photo-z data all galaxies have a weight equal to 1, and using the modified test is equivalent to using the standard one.

5.1 The total mass function and its evolution

We first compare the mass distribution of all galaxies at low and high redshift. As we are interested in the shapes of the mass functions and not in the total number of galaxies, we normalize the mass distribution of EDisCS galaxies to the mass distribution of WINGS galaxies to have the same total number of galaxies above $\log M_*/M_\odot \geqslant 11$. In this way we assume that the most massive galaxies are already in place at z$\sim$ 1 (see, e.g., Fontana et al. 2004; Pozzetti et al. 2007).

In Figure 6 the mass distribution of WINGS galaxies (crosses) is compared to the mass distribution of EDisCS galaxies (squares). The comparison is meaningful only above the highest of the two mass completeness limits, that is for $\log M_*/M_\odot \geqslant 10.2$.

The two mass distributions are very different. Indeed, the EDisCS mass function is flat for $\log M_*/M_\odot \leqslant 10.8$. The WINGS mass function is rather flat up to about $\log M_*/M_\odot \sim 10.6$ and then

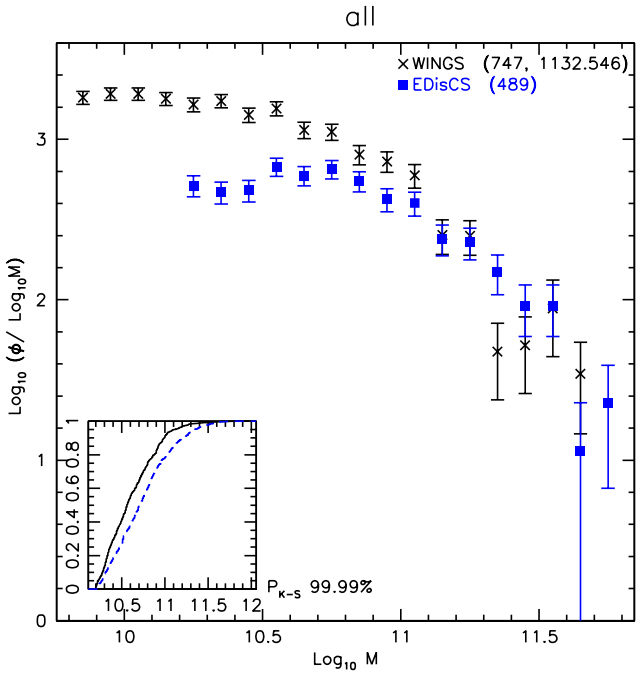

Figure 6. Comparison of the mass distribution of EDisCS (blue filled squares) and WINGS (black crosses) galaxies of all morphological types, for the mass limited sample. Mass distributions are normalized to have the same total number of objects at $\log M_*/M_\odot \geqslant 11$. Errors are poissonian. Only points above the respective completeness limits are drawn. Numbers in the labels are the total number of galaxies above the highest of the two completeness limits. For WINGS, both observed (first) and weighted (second) numbers are given. The inset shows the cumulative distributions, with the relative K-S probability, for galaxies above the common mass limit. The mass distributions depend on redshift: for a similar number of higher mass galaxies, for $\log M_*/M_\odot \leqslant 10.8$ there are proportionally less massive galaxies at low-z than at high-z.

it begins to decline more steeply, with a massive end slope similar to that of the EDisCS mass function. The striking difference is the dearth of galaxies less massive than $\log M_*/M_\odot \leqslant 10.8$ in EDisCS compared to WINGS, for the same number of massive galaxies. The K-S test confirms that the two distributions are different at the 99.99% level. We remind that the results of the K-S test do not depend on the normalization we adopted in the plots. So, also using other normalization criteria, we would reach the same conclusions.

We conclude that the total mass distribution of galaxies in clusters evolves with redshift. In a mass-limited sample, cluster galaxies at high-z are on average more massive than in local clus-

ters. Assuming no evolution at the massive end, the population of $\log M_*/M_\odot \leqslant 10.8$ galaxies must have grown significantly between $z = 0.8$ and $z = 0$.

In principle, the evolution of the galaxy stellar mass function can be due to several factors: a) strong environmental mass segregation, for which galaxies infalling into clusters between the two redshifts have a different mass distribution than galaxies already in clusters at high-z (infalling galaxies being on average less massive); b) mass loss from massive galaxies due to harassment; c) galaxy merging; d) mass growth due to star formation. In §7 we will discuss which effects are likely to play an important role and which ones can probably be neglected in this study.

5.2 The mass functions of different galaxy types

We now analyze separately the mass function of each morphological type, to see if and how the distribution of masses depends on the galaxy type. In this case, we do not apply any normalization among the different mass functions, to show what morphological type dominates as a function of mass. Figure 7 shows the mass distributions for galaxies of the WINGS dataset (left panel) and of the EDisCS dataset (right panel). Galaxies of different morphological types are indicated by different colors and symbols.

In Table 4 we give the analytic expression for the mass functions of the different morphological types for both samples, estimating the best-fit Schechter (1976) parameters (α, M^*, ϕ^*).

For WINGS, the shape of the mass distribution strongly depends on morphological type. The total mass function is dominated by S0 galaxies up to $\log M_*/M_\odot \sim 11$, and by elliptical galaxies at higher masses. The total mass function is quite flat up to $\log M_*/M_\odot \sim 10.6$, as it is the function of both S0s and ellipticals. Instead, the mass function of late-type galaxies declines over the whole mass range. While there are elliptical galaxies at all masses, there are no S0s or late-types more massive than $\log M_*/M_\odot \sim 11.4$ and $\log M_*/M_\odot \sim 11.6$ respectively.

We perform a K-S test, both for a mass limit $\log M_*/M_\odot \geqslant 9.8$ (the WINGS limit), and for $\log M_*/M_\odot \geqslant 10.2$ (the same limit as EDisCS). The K-S results are summarized in Table 5.[5]

For $\log M_*/M_\odot \geqslant 9.8$, the morphological mass functions significantly differ one from another: ellipticals, S0 and late-type galaxies all have different mass functions, with the K-S that excludes the possibility that they are drawn from the same parent distribution with a probability always greater than 99.4%. For $\log M_*/M_\odot \geqslant 10.2$, S0s and late-type galaxies are not statistically distinguishable any more (probability = 91.4%). This suggests that, except for the least massive galaxies, the S0 and spiral mass functions could in fact be similar. This could be due to the fact that when we analyze the sample at $\log M_*/M_\odot \geqslant 10.2$ we are actually excluding Sc and Irregulars galaxies, that mostly have masses below this limit. However, in our sample, they represent only 5% of the total population of late-type galaxies, so we do not expect they matter a lot.

Comparing each type with all galaxies, for $\log M_*/M_\odot \geqslant 9.8$ only S0 galaxies could have a similar distribution to the sum of all galaxies ($P_{K-S} \sim 70\%$), while in the other two cases the test indicates that the distributions are different, with a probability at least $> 98.5\%$. Instead, above $\log M_*/M_\odot = 10.2$ the K-S test is less conclusive: it rejects the hypothesis of similarity only between ellipticals with all galaxies, with a probability of 99.9%. This demonstrates how important it is to reach deep mass limits: in fact the greatest differences among the mass functions tend to emerge at lower masses.

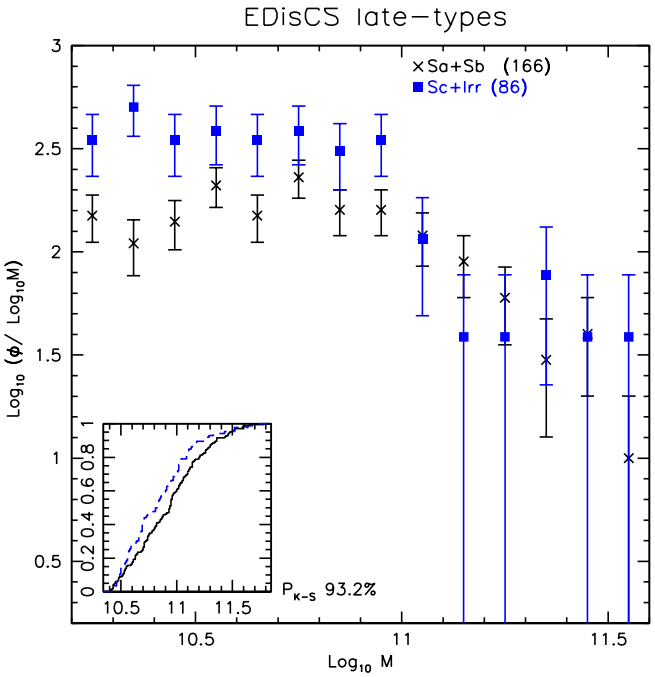

Figure 8. Mass distribution of EDisCS late galaxies split into Sa+Sb (black crosses) and Sc+Irr (blue filled squares), for the mass limited sample. Mass distributions are normalized to have the same total number of objects at $\log M_*/M_\odot \geqslant 11$. Errors are poissonian. Numbers in the labels are the total number of galaxies above the completeness limits. The inset shows the cumulative distributions, with the relative K-S probability, above the common mass completeness limit. The two distributions are quite different, indicating that early- and late-spirals have different mass distributions.

For EDisCS (right panel in Figure 7), the total mass function is dominated by the mass function of late-type galaxies up to $\log M_*/M_\odot < 11$ (and not by S0s galaxies as in WINGS). The most massive bins of the total function are dominated by elliptical galaxies. In fact, there are no S0s or late-types more massive than $\log M_*/M_\odot \sim 11.5$ and $\log M_*/M_\odot \sim 11.6$ respectively. The mass function of S0s is very noisy, due to their low number in the sample.

At high-z, the data cannot rule out that the mass functions of the different morphological types are all similar, with K-S probabilities always smaller than or at most equal to 90% (see Table 5). We also split late-type galaxies in Sa+Sb and Sc+Irr galaxies, to investigate if the two populations behave differently (Figure 8). Even though the K-S seems to be not conclusive (it gives a probability of $\sim 93\%$), we find that mass functions are quite different (Figure 8), indicating that there are proportionally more lower mass galaxies ($\log M_*/M_\odot < 11$) among Sc+Irr than among Sa+Sb.[6]

Also the comparison between each morphological type and all

[5] We note that with the term "all" we refer to all galaxies regardless of their morphological type and we are including also galaxies for which we do not have a morphological classification, that are only a few (see Table 3). However, we have checked that the mass distribution is the same considering all galaxies or only the sum of ellipticals, S0s and late-type galaxies.

[6] We note that such an analysis cannot be performed in WINGS, due to the very small number of Sc+Irr.

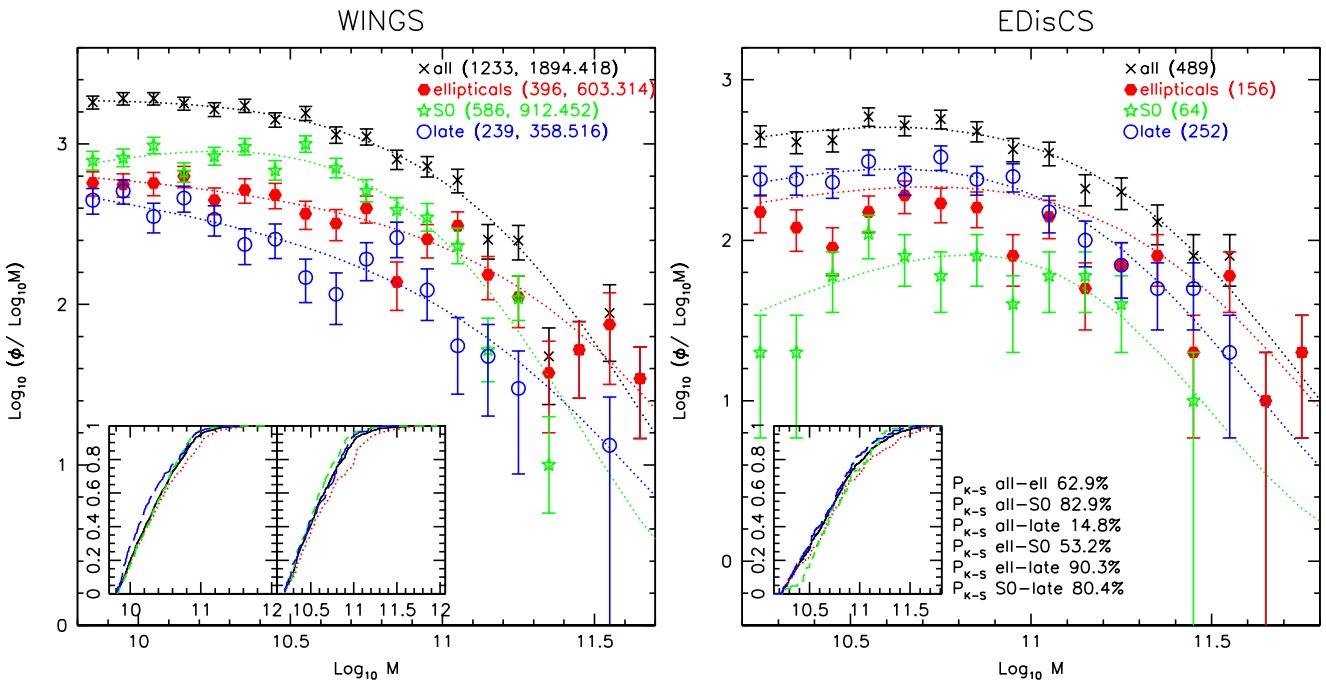

Figure 7. Mass distribution of WINGS galaxies (left panel) and EDisCS galaxies (right panel). In the insets, the cumulative distributions are shown. For WINGS, the right inset is done for the EDisCS mass limit, $\log M_*/M_\odot$ = 10.2. Black crosses represent all galaxies, filled red circles elliptical galaxies, green stars S0s and blue open circles late-type galaxies. Errors are defined as poissonian errors. Numbers in the labels are the number of galaxies in each morphological class, above the respective mass limit. For WINGS, both observed (first) and weighted (second) numbers are given. For EDisCS, the K-S probabilities are also given. Best-fit Schechter (1976) mass function are showed dotted. The values of the parameters of the fit are presented in Table 4. At low-z, different morphological types have different mass functions, while at high-z no conclusion can be drawn.

		$\log M^*$	α	ϕ^*
WINGS	all galaxies	11.667±0.052	-0.987±0.009	1.552±0.055
	early-types	11.643±0.055	-0.977±0.011	1.526±0.059
	ellipticals	11.879±0.076	-1.017±0.014	1.13±0.067
	S0s	11.391±0.052	-0.925±0.020	1.680±0.089
	late-types	11.683±0.171	-1.04±0.031	0.992±0.138
EDisCS	all galaxies	11.684±0.061	-0.915±0.026	1.577±0.105
	early-types	11.700±0.081	-0.896±0.041	1.423±0.138
	ellipticals	11.847±0.126	-0.947±0.044	1.159±0.148
	S0s	11.300±0.125	-0.662±0.147	1.679±0.235
	late-types	11.523±0.067	-0.875±0.044	1.560±0.141

Table 4. Best-fit Schechter (1976) parameters (α, M^*, ϕ^*) for the galaxy mass functions of the different morphological types discussed in this paper. Fits are perfomed directly on the logarithmic points.

	WINGS		EDisCS
	P_{K-S} ($M_* \geqslant 10^{9.8} M_\odot$)	P_{K-S} ($M_* \geqslant 10^{10.2} M_\odot$)	P_{K-S} ($M_* \geqslant 10^{10.2} M_\odot$)
ell-S0	99.84%	99.99%	53.18%
ell-late	99.44%	98.20%	90.20%
S0-late	99.72%	91.40%	80.43%
all-ell	99.38%	99.9%	62.98%%
all-S0	69.52%	95.53%	82.89%
all-late	98.64%	24.94%	14.77%

Table 5. Results of the Kolmogorov-Smirnov test performed on the mass function of different morphological types for the WINGS and EDisCS mass limited sample. For WINGS, results also above the EDisCS mass completeness limit are given. P_{K-S} is the probability that two distributions are drawn from different parent distributions. The K-S has been modified to take into account the different weights of galaxies observed spectroscopically.

galaxies does not give conclusive results, because the K-S probabilities are always smaller than 90%. In WINGS, we have seen that, for the same mass limit, only S0s and late-types could have the same mass distribution, while they both differ from ellipticals. The lack of significance of the differences in EDisCS might be due to poorer number statistics, as well as to the higher mass limit.

To check if the lack of significance in EDisCS is real or above all due to poor statistics, we performed 100 Monte Carlo simulations extracting randomly from the WINGS sample at $\log M_*/M_\odot \geqslant 10.2$ a subsample with the same number of galaxies as EDisCS (that is 156 ellipticals, 64 S0s and 252 spirals). We found that the probability of the K-S test to be conclusive is very low in all cases (at most in 56% of the simulations when we compare ellipticals and late-types). These results are consistent with the hypothesis that in EDisCS the lack of a significant difference between the mass functions of different types could be due to poor number statistics.

The conclusion we can draw from this section is that, at low redshift, different morphological types have significantly different mass functions, although S0s and late-type galaxies more massive than $\log M_*/M_\odot = 10.2$ may have similar mass distributions. No conclusion can be drawn at high redshift.

5.3 Evolution of the mass functions of different morphological types

We now directly compare the mass distribution of each morphological type in the two reshift bins, with the aim to understand if the shape of the mass function of each given type evolves with redshift, and what type of galaxies drives the evolution of the total mass function. As for the total mass function, we normalize the mass distribution of EDisCS galaxies to the mass distribution of WINGS galaxies to have the same total number above $\log M_*/M_\odot \geqslant 11$, since we want to compare the shape of the distributions.

Figure 9 compares the mass distribution of galaxies of each morphological type at high and low redshift. The mass distribution of ellipticals is shown in the top left panel. For both WINGS and EDisCS, the mass distribution starts rather flat at low masses, with a hint for a possible dip in EDisCS, then begins to steepen at higher masses. Statistically, the EDisCS and WINGS distributions are significantly different. As for the total mass function, there is a deficit of less massive galaxies ($\log M_*/M_\odot \leqslant 10.6$) at high-z compared to low-z, for a given number of more massive galaxies. A K-S test rejects the null hypothesis of similarity of the two distributions with a probability >99.9%.

In the top right panel of Figure 9 the mass distribution of S0 galaxies is shown. It changes dramatically with redshift. WINGS galaxies have a flat mass function up to $\log M_*/M_\odot \sim 10.6$ and then this becomes steeper. Instead, the mass function of EDisCS galaxies shows a rise, a peak at about $\log M_*/M_\odot \sim 10.6$, and a fall. The K-S test states that the mass distributions at the two redshifts are driven from two different parent distributions with a probability $> 99.99\%$. This result emerges with a high statistical significance even though S0 galaxies are very rare in the EDisCS sample.

In the bottom left panel of Figure 9 we analyze the mass function of early-type galaxies. This can be directly compared with the mass function of late-types (bottom right panel). The differences existing in the total mass distribution still remain evident in the mass function of early-type galaxies. While the mass distribution of high mass galaxies is rather similar at the two redshifts, the dearth of galaxies with $\log M_*/M_\odot \leqslant 10.9$ in EDisCS is even more evident than in the total mass function. Once again, the K-S test rejects the possibility that the two mass functions derive from the same distribution with a probability >99.9%. Of course, this behavior was expected, being the early-type galaxies simply the sum of ellitpicals and S0s.

The bottom right panel of Figure 9 shows the mass distribution of late-type galaxies. The shape of the mass distribution of EDisCS and WINGS is different up to $\log M_*/M_\odot \sim 11$ and then it is rather similar at higher masses. For WINGS late-types, the mass distribution is immediately declining, while that of EDisCS starts flat. The K-S test gives a probability of $\sim 98\%$ that the two distributions are not driven from the same parent distribution.

The conclusion we can draw from this section is that the mass distribution of *each* morphological type evolves with redshift. All types have proportionally more massive galaxies at high- than at low-z.

In addition to the processes mentioned in §5.1 (infall, harassment, merging and star formation) that can change the total mass function, there is an additional effect that could influence the observed evolution of the mass functions of each morphological type: the morphological transformation from one type to the other.

6 RESULTS: THE MORPHOLOGICAL FRACTIONS

6.1 The Morphology-Mass relation

It is interesting to analyze how the incidence of each morphological type (the number of galaxies of that type over the total) changes as a function of the stellar mass (hereafter the morphology-mass relation, MMR).

As in the following we will compare our findings with the results found by Desai et al. (2007) and Poggianti et al. (2009) that use magnitude limited samples, we discuss the MMR both in mass limited and in magnitude limited samples. Since above the completeness limit of our samples the fraction of objects without morphological classification is negligible (at most 4%) in this analysis we do not consider them, so we refer to "all" galaxies simply as the sum of early and late-type galaxies.

Figure 10 shows the fractions of the different morphological types as a function of galaxy mass, for both EDisCS and WINGS. In the left panel, the mass limited samples are presented. Errors are defined as binomial errors (Gehrels 1986).

The trend of ellipticals at high and low redshift is similar: the elliptical fraction is flat at low masses, then it increases at higher masses. Ellipticals represent more than 50% of galaxies at any mass greater than $\log M_*/M_\odot \sim 11$ at low-z and $\log M_*/M_\odot \sim 11.4$ at high-z. Thus, WINGS elliptical galaxies start to dominate at a lower mass than in EDisCS. The most massive galaxies tend to be almost all ellipticals, at both redshifts.

The morphology-mass relation of S0s and late-types galaxies depends even more strongly on redshift. In the Local Universe, for masses up to $\log M_*/M_\odot \sim 11$ S0s are by far the most common galaxies, and their fraction is rather constant with mass up to $\log M_*/M_\odot \sim 10.9$, whereas it decreases steeply towards higher masses. In contrast with the local Universe where S0s are much more frequent at low than at high masses, at high-z S0s are equally rare ($\leqslant 20\%$) at all masses.

Late-type galaxies are the least represented morphological class in the Local Universe ($\leqslant 20\%$ at all masses), their trend hardly depending on mass (excluding a possible fluctuation at $\log M_*/M_\odot \sim 10.9$). At higher redshift, the situation is different: late-types are the most common type of galaxies up to

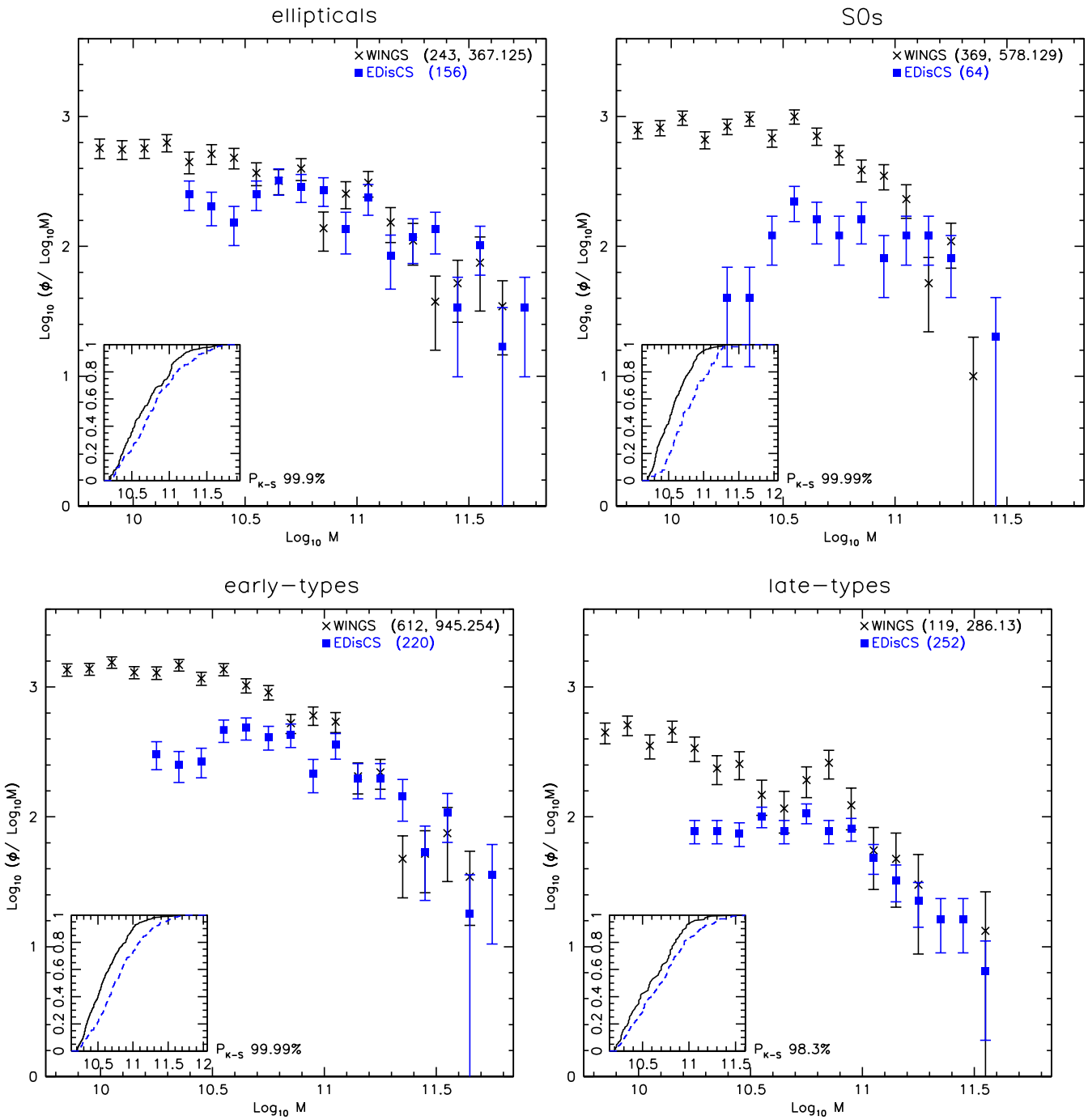

Figure 9. Comparison of the mass distribution of EDisCS (blue filled squares) and WINGS (black crosses) galaxies, for the different morphological types. Mass distributions are normalized to the WINGS total number of objects with $\log M_*/M_\odot \geqslant 11$. Errors are defined as poissonian errors. Numbers in the labels are the number of galaxies in each morphological class, above the respective mass limit. For WINGS, both observed (first) and weighted (second) numbers are given. The cumulative distributions are shown in the insets. Each morphological type has a mass distribution that depends on redshift. In WINGS there are always proportionally more less-massive galaxies than in EDisCS.

$\log M_*/M_\odot \sim 11.3$, with no clear trend with mass at lower masses, and a steep decline at higher masses.

In magnitude limited samples, the dependence of the morphological fractions on mass is even more pronounced, at both redshifts. At low masses, late-type galaxies dominate the total population, while the presence of elliptical galaxies is negligible. On the contrary, at higher masses elliptical galaxies are the most numerous, and late-type galaxies the least numerous type of galaxies. As far as S0s are concerned, while in WINGS they dominate at intermediate masses ($\log M_*/M_\odot \sim 10.1-10.9$), in EDisCS they do not dominate at any mass. Comparing high and low redshift, in general there are many more intermediate-mass and massive EDisCS late-types than WINGS late-types, that instead dominate only the first bins up to $\log M_*/M_\odot \sim 10.1$, and then fall to

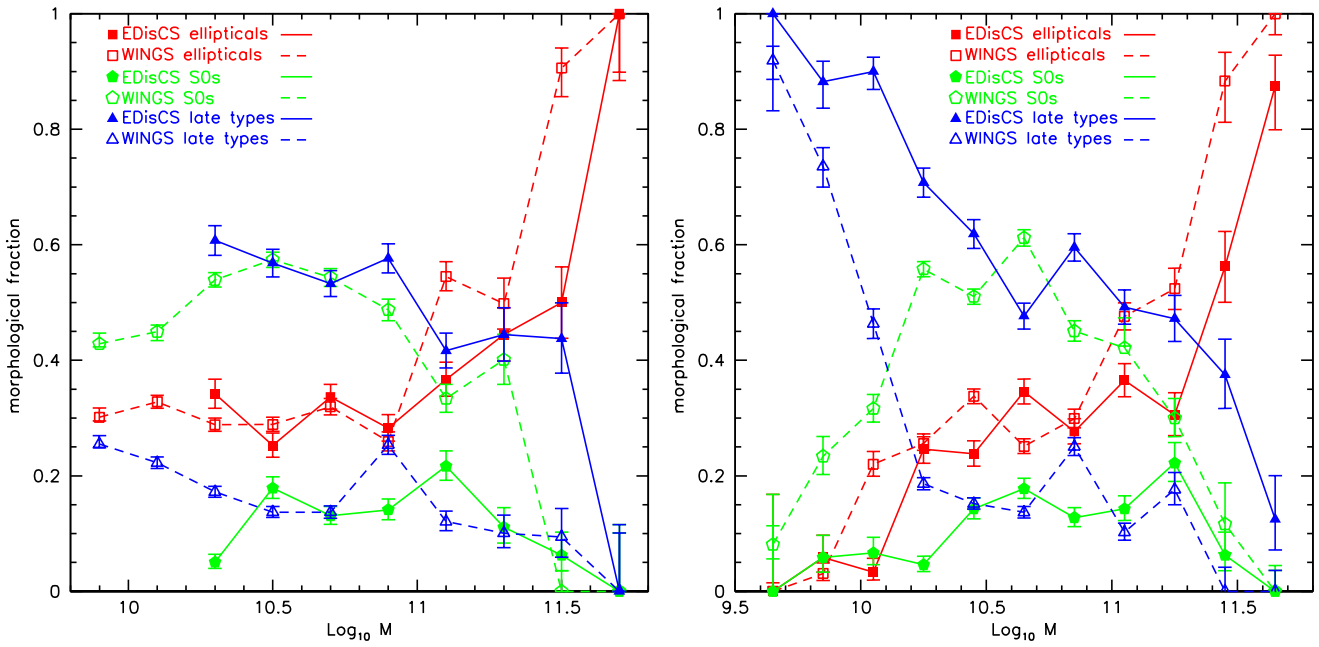

Figure 10. Morphological fractions for the mass limited (left panel) and magnitude limited (right panel) samples for galaxies at different redshifts. Solid symbols and lines refer to EDisCS, empty symbols and dotted lines refer to WINGS. Squares refer to ellipticals, circles refer to S0s, triangles refer to late-types. Errors are defined as binomial errors. In both samples, the morphological mix changes with galaxy stellar mass and with redshift at a given mass (see text for details).

zero by $\log M_*/M_\odot \sim 11.5$. Similarly to the mass-selected sample, WINGS ellipticals start to dominate at lower masses than in EDisCS.

These results show how the proportion of galaxies of different morphological types changes with galaxy mass. This MMR is significantly different in our mass-limited and magnitude-limited samples. In the mass-limited sample, the incidence of each type *does not depend on mass* between our completeness mass limits and $\log M_*/M_\odot \sim 11-11.1$ (flat trend), while it strongly changes at higher masses. Both for the mass-limited and the magnitude-limited samples, the MMR evolves strongly with redshift, in connection to the evolution of the morphological fractions described below.

6.2 Evolution of morphological fractions

The morphological fractions for both mass and magnitude limited samples are given in Table 6. WINGS fractions are given also above the EDisCS mass limit. For WINGS, fractions are computed both for unweighted and for completeness-weighted numbers. We can note that the completeness correction does not change the resulting fractions significantly.

Except for late-types, in WINGS, fractions of different morphological types do not depend on the choice of the mass limit, remaining constant within the errors. Moreover, the choice of the sample (mass or magnitude limited) does not alter the trends observed.

The fraction of elliptical galaxies does not change with redshift, being almost constant ($\sim$ 30%). Instead, the fraction of S0 and late-type galaxies considerably changes, being S0s much more common in the Local Universe, while spirals are proportionally less common.

	WINGS $M_V \leqslant -19.5$ (Poggianti et al. 2009)	EDisCS $M_V \leqslant -20$ (Desai et al. 2007)
ellipticals	$33 \pm 7\%$	$29 \pm 1\%$
S0s	$44 \pm 10\%$	$14 \pm 1\%$
early-types	$77 \pm 12\%$	$43 \pm 2\%$
late-types	$23 \pm 9\%$	$57 \pm 3\%$

Table 7. Morphological fractions obtained from Poggianti et al. (2009); Desai et al. (2007).

As a consequence, the early-type fractions strongly evolves, almost doubling from high- to low-z. This is in agreement with the finding of Kovac et al. (2009) for the field, but it is in contrast with Holden et al. (2007), who find no evolution in the early-type fraction in clusters from $z \sim 0.8$ to the current epoch in a mass limited sample with $\log M_*/M_\odot \geqslant 10.55$. Our trend still remains outstanding ($\sim$ 50% at z$\sim$ 0.8 and $\sim$ 83% at z$\sim$ 0) even if we adopt the Holden et al. (2007) mass limit.

Our results are in very good agreement with those found previously by Poggianti et al. (2009) and Desai et al. (2007) for the WINGS and EDisCS datasets, respectively, listed in Table 7.

We note that here we use only spectroscopic members in a subset of 21 WINGS clusters, while Poggianti et al. (2009) used all galaxies in the photometric catalog of 72 WINGS clusters. Moreover, we note that considering EDisCS photo-z members, our fraction are in perfect agreement with those found by Desai et al. (2007), who used the total photometric catalog and a statistical background-subtraction technique, indicating that photo-z techniques to assign membership and statistical subtraction give consistent results.

	WINGS						EDisCS	
	$M_* \geqslant 10^{9.8} M_\odot$		$M_* \geqslant 10^{10.2} M_\odot$		$M_V \leqslant -19.5$		$M_* \geqslant 10^{10.2} M_\odot$	$M_V \leqslant -20$
	$\%_{obs}$	$\%_w$	$\%_{obs}$	$\%_w$	$\%_{obs}$	$\%_w$	%	%
ellipticals	32.4±1.3%	32.2±1.1%	33.2±1.7%	32.7±1.4%	30.4±1.6%	30.0±1.3%	33.0±2.2%	28.9±2.0%
S0s	48.0±1.4%	48.7±1.2%	50.5±1.9%	51.5±1.5%	47.4±1.7%	48.4±1.4%	13.6±1.6%	12.8±1.5%
early	80.4±1.1%	80.9±0.9%	83.7± 1.4%	84.2±1.1%	77.8±1.4%	78.4±1.1%	46.6±2.3%	41.8±2.1%
late-types	19.6±1.1%	19.1±0.9%	16.3±1.4%	15.8±1.1%	22.2±1.4%	21.6±1.1%	53.4±2.3%	58.2±2.1%

Table 6. Morphological fractions of galaxies in both mass and mag-limited samples. Errors are computed as binomial errors. For WINGS, both observed and completeness-weighted numbers are listed. Since galaxies with unknown morphology are always $\leqslant 4\%$, they are not included in the computation of fractions.

	WINGS		EDisCS
	$M_* \geqslant 10^{9.8} M_\odot$	$M_* \geqslant 10^{10.2} M_\odot$	$M_* \geqslant 10^{10.2} M_\odot$
ellipticals	$42 \pm 4\%$	$43\pm 5\%$	$39 \pm 5\%$
S0s	$42 \pm 4\%$	$42 \pm 4\%$	$13 \pm 2\%$
early-types	$84 \pm 6\%$	$85 \pm 7\%$	$52 \pm 5\%$
late-types	$16 \pm 2\%$	$15 \pm 2\%$	$46 \pm 4\%$
unknown	$0.63 \pm 0.22\%$	$0.54 \pm 0.24\%$	2 ± 1 %

Table 8. Fraction of mass in galaxies of each type, above the different limits for WINGS and EDisCS. Errors are calculated with the propagation of errors, assuming a mean error on each galaxy mass equal to the mass itself.

6.3 In what type of galaxies is most of the mass?

In Table 8 we present the amount of mass in each morphological type, to quantify the relative contribution of each class to the total stellar galaxy mass. We stress that only galaxies more massive than our mass limits are considered, and no attempt is made to extrapolate to lower galaxy masses to obtain the total mass, integrated over all galaxy masses.

Errors are calculated with the propagation of errors, assuming a mean error on each galaxy mass equal to the mass itself, which corresponds to the 0.3 dex error in mass discussed in §3.

At low redshift, for $\log M_*/M_\odot \geqslant 10.2$, $\sim 85\%$ of the mass is in early-type galaxies, of which half in S0s and half in ellipticals. At high redshift, only about 50% of the mass is in early-type galaxies, of which most ($\sim 3/4$) is in ellipticals.

Interestingly, the fraction of stellar mass in WINGS S0s is the same as in EDisCS late-types. So it is not just the number fraction of high-z spirals (S0s) that matches that of low-z S0s (spirals), but also the mass fractions. Consequently, it is not just the number fraction of ellipticals that remains constant with redshift (see previous section), but also the fraction of mass in ellipticals, being about 40% both in EDisCS and in WINGS.

7 DISCUSSION

In this paper, we have presented mass functions both of all galaxies and of different morphological types in clusters at different epochs.

For a high mass threshold ($\log M_*/M_\odot \sim 11$), the shapes of our $z = 0.7$ and $z = 0.05$ mass functions are similar, consistent with high-mass galaxies having already established their mass at high-z. The K-S test supports this assumption, giving a probability $\sim$ 90% that the two distributions are not driven from the same parent distribution.

This is in agreement with results for the field, where for example, Bundy et al. (2006) and Franceschini et al. (2006) found that the high-mass end of the mass function is quite constant at least from $z \sim 1$ to $z \sim 0$. This is also in agreement with previous studies of the bright end of the galaxy luminosity function in clusters at red wavelengths (De Propris et al. 2007, Toft et al. 2004, Andreon 2006).

In contrast, going to less massive galaxies, the differences increase: clusters in the local Universe have proportionally many more less-massive galaxies than clusters in the distant Universe.

We have found the same when the sample is divided by morphological type. Furthermore, we have shown how the morphological mix changes with galaxy stellar mass, and with redshift at a given mass.

Both the number fraction and the mass fraction of ellipticals does not change with z, while the fractions of S0s and spirals are inverted at the two redshifts.

At the end of §5.1 and 5.3 we have identified some mechanisms that in principle could contribute to the observed evolution of the mass functions and of the morphological mix.

In this section, we discuss each one, trying to understand which ones can be the most relevant in driving the trends observed.

- *merging*: a galaxy can gain mass through mergers with other galaxies; so mergers could drive both galaxy mass assembly and dynamical evolution in a hierarchical scenario. However, in clusters this process is not expected to play an important role (see e.g. Ostriker 1980; Makino & Hut 1997; Mihos 2004): the high velocity dispersions in clusters suppress mergers (see e.g. Ellison et al. 2010 and references therein). More importantly, this type of process should favor the growth of the high-mass end of the mass function relative to the low-mass end, as we observe. Finally, visual morphological classifications show that the fraction of colliding galaxies in clusters is low (e.g. Desai et al. 2007).
- *harassment*: galaxies in clusters are subject to frequent high speed encounters that strip a galaxy of part of its mass and drive a morphological transformation. Harassment has the potential to change any internal property of a galaxy within a cluster including the gas distribution and content, the orbital distribution of stars and the overall shape (Moore et al. 1996). Its strength depends on the collisional frequency, on the strength of the individual collisions, on the cluster's tidal field and on the distribution of the potential within galaxies. It has long timescales since it needs multiple encounters to be efficient in removing gas and stars and quenching star formation. It effectively perturbs low-mass galaxies while its effects on massive objects should be less pronounced (Moore et al. 1996; Boselli & Gavazzi 2006).
- *environmental mass segregation of infalling galaxies:* clusters are far from being closed boxes, so the infall of galaxies from surrounding areas is a mechanism that certainly takes place. If galaxies surrounding the clusters have a steeper mass function than the

cluster, they would make a greater contribution to the total mass function at intermediate to low-masses.

Characterizing this process is very complex, since there are several factors that must be understood. a) First of all, we should know the rate of infalling galaxies with time, to understand how the number of galaxies in clusters increases with redshift. b) Then, we should know the relative fraction of the different morphological types of infalling galaxies. It depends on the morphological mix of galaxies located in the surrounding areas the clusters. In the field the morphological mix evolves with redshift (Pannella et al. 2006), so we also need the proportions of the morphological types of infalling galaxies to change from $z \sim 0.8$ to $z \sim 0$ (though van der Wel et al. (2007) find that the early-type fraction in the field and group environments is quite constant ($\sim$45%) from $z \sim 0.8$ to the current epoch). In the outskirts of the cluster, the global morphological mixing is correlated with local density (e.g. Huertas-Company et al. 2009). In general, in the field there are more late-type galaxies than early-types (at $z \sim 0.6$, $\sim 70\%$ at low masses, $\geqslant 50\%$ at intermediate masses (Oesch et al. 2010)) so late type galaxies are probably the favourite infalling galaxies. c) Most importantly, we should know the exact mass distribution of infalling galaxies, that can be expected to differ from that of galaxy clusters. For example, Baldry et al. (2006) and Bolzonella et al. (2009) found a dependence of the mass function on the local density. However, as we will show later, comparing field and cluster galaxy mass functions, there seem to be no large differences in the different environments (see §7.2).

- *star formation*: galaxies can increase their stellar mass forming new stars. The fraction of star-forming galaxies is of course much lower in clusters than in the field at the same redshift (Finn et al. 2010). At least at intermediate redshifts, the star formation rate in star-forming cluster galaxies is similar to that of field star-forming galaxies of the same mass, except for a 10% population of cluster star-forming galaxies with reduced star formation rates (Vulcani et al. 2010). For the field, Oesch et al. (2010) have found that the latest types of galaxies (bulge-less and irregulars) show a non-negligible mass growth over the time span from $z \sim 0.9$ to $z \sim 0.3$, while in earlier types internal star-formation since $z \sim 0.9$ only results in a negligible increase (<1%) in the stellar mass.
- Finally, when considering the evolution in the mass functions of each morphological type, it is relevant to keep in mind that galaxies can be subjected to a *morphological transformation*, that is a change in their morphological type, either simply due to passive evolution or due to influences by other processes. Infalling galaxies meet a new environment that can alter their properties and they are subject to several mechanisms that e.g. can quench their star formation processes.

From these descriptions, we can conclude that merging does not play an important role in driving the evolution of the mass functions we observe.

In principle, harassment could modify the shape of the mass distribution, and influence the mass function of each morphological type, altering the galaxy morphology. However, since it is more and more efficient at lower masses, we would expect it to decrease the number of low mass galaxies at lower redshifts, therefore to produce the opposite effect of what we observe (and might have to be "overcome" if harassment is an important process). Thus, even if it could contribute in shaping and modifying the mass function, harassment does not provide a satisfactory explanation for our findings.

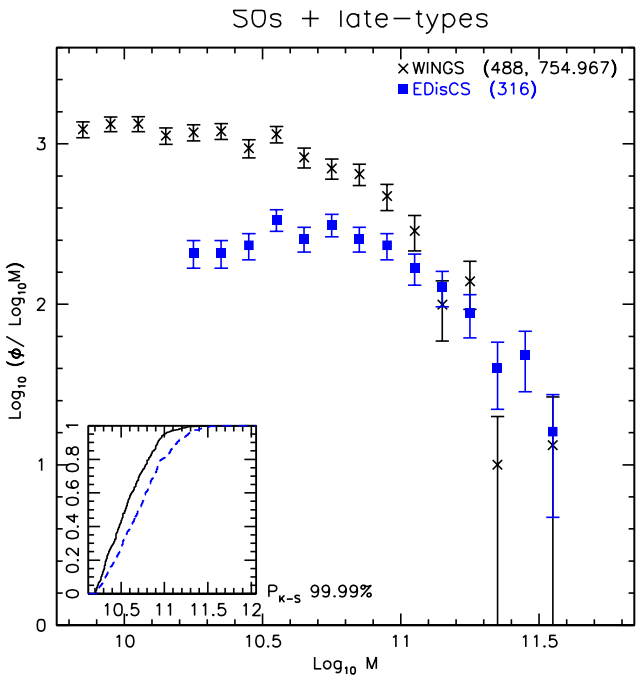

Figure 11. Comparison of the mass distribution of EDisCS (blue filled squares) and WINGS (black crosses) S0+late-type galaxies. Mass distributions are normalized to have the same total number of objects at $\log M_*/M_\odot \geqslant 11$. Errors are poissonian. Numbers in the labels are the total number of galaxies above the respective mass completeness limit. For WINGS, both observed (first) and weighted (second) numbers are given. In the insets the cumulative distributions are shown.

The other mechanisms listed above could play an important role in driving the observed evolution in clusters, so in the following, we try to quantify separately the extent of the possible contribution of each one.

7.1 The role of the morphological transformations

The infall of galaxies certainly occurs at each redshift, however it is hard to quantify its extent. Hence, in this section, we wish to test if morphological transformations from one type to another, alone, can explain the evolution of the mass function of the various morphological types, neglecting any other possible effect, assuming that the rate of morphological evolution does not depend on galaxy mass and considering clusters as closed boxes. In this section we only consider mass-limited samples.

Since both the mass fraction and the number fraction in elliptical galaxies remain quite constant with redshift (as seen also in Table 3), let us at first assume that the only efficient mechanism is one that transforms a late-type into an S0 galaxy. If this were the case, the mass distribution of late+S0 galaxies should not change with time. Instead, Figure 11 shows that it is very different at the two redshifts ($P_{K-S} > 99.9\%$), indicating that the evolution of the mass functions cannot be explained simply by turning late-type galaxies into S0s and neglecting infall and any other mechanism.

In the next step, we recreate a more complex situation, including elliptical galaxies in our analysis too and making the hypothesis that, still in a closed box, observed early-types in WINGS derive from early-types in EDisCS and from a fraction of EDisCS late-types that changed their morphology to earlier types.

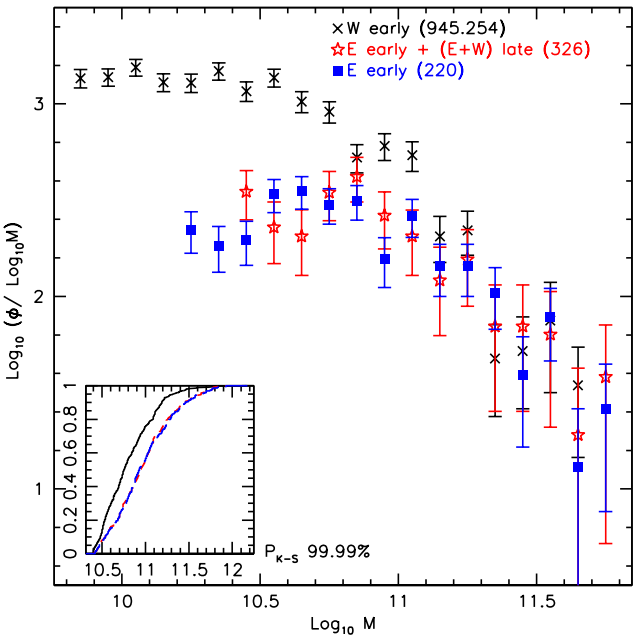

Figure 12. Model of a possible evolution of the mass functions without taking into account the infall of galaxies from areas surrounding the clusters. Black crosses: observed WINGS early-types, Blue filled squares: observed EDisCS early-types (same as third panel Figure 9). Red stars: simulated mass function of WINGS early-types assuming they derive simply from all EDisCS early-types, and from some of the EDisCS late-types (see §6.4 for details).

In practice, since we hypothesize a closed system, we have to assume that the fraction of early-types in WINGS (84%) has to be equal to the fraction of early-types in EDisCS (47%) plus some of the late-type galaxies in EDisCS necessary to maintain the right proportions (X times the late-type fraction = X times 58%). We determine this quantity assuming that the total number of galaxies cannot change and hence X must be equal to 0.64.

We find (Figure 12) that the resulting simulated mass function is very different from the observed early-type WINGS mass function, indicating that the early-types in WINGS cannot derive simply from the evolution of late-types of EDisCS, no infall and no other mechanism at work. The K-S test support what is clear from the figure, giving a probability $> 99.99\%$ that the distributions do not derive from the same parent one.

Hence, it is impossible to reconcile the mass functions observed at low-z with a simple picture in which there is no infall, each galaxy type preserves its mass distribution unaltered and late-type galaxies are turned into early-types by some mechanism that leaves their stellar mass unaltered.

While morphological transformations are likely to occur, they have to be accompanied by other mechanisms to explain the observed trends.

7.2 Can infalling galaxies explain the observed evolution?

Environmental mass segregation in infalling galaxies could play an important role, for the reasons discussed in previous sections, but we have no means to assess its role without knowing the infall rate, mass distribution and morphological mix of accreting galaxies.

In the literature, there are few works in which the mass distributions of galaxies of different morphological types are presented. Ilbert et al. (2010) analyzed the evolution from $z = 2$ to $z = 0$ for different morphological and spectral types in the field using the COSMOS 2 deg^2 field; in the following, we will consider their mass distribution of elliptical and all galaxies in the redshift bin $0.6 \leqslant z \leqslant 0.8$. Bundy (2005)[7], analyzed both together and separately, for the early- and late-type field galaxies in the GOODS fields in the redshift range $0 < z < 1$. In the following, we will also consider their data between $0.55 \leqslant z \leqslant 0.8$ as reference.

First of all, we wish to compare the total mass functions. Figure 13 shows the comparison between cluster and field mass functions for all galaxies, above the common mass limit, that is $\log M_*/M_\odot \sim 10.3$ once all masses have been converted to the same IMF. The mass functions are normalized in order to have the same total number of galaxies above $\log M_*/M_\odot \geqslant 11$.[8]

We see that at high masses ($\log M_*/M_\odot \geqslant 11$), the mass function of field and cluster galaxies at high-z show a rather similar shape. However, since we are trying to understand the reasons of the observed differences between the mass functions at different redshifts in the lower massive tail, where WINGS and EDisCS give different results, we are more interested in comparing the shape of the mass function of galaxies at intermediate and low masses, assuming the massive tail to be fixed.

As Figure 13 illustrates, the two field studies we adopted for comparison give quite different results at these masses. If we followed Ilbert et al. (2010) (blue dashed line), we could suggest that field galaxies have a steeper mass function than cluster galaxies, indicating the presence of a significant environmental mass segregation. In this way, the infall of galaxies from the field could be at least partly responsible for the growth of the low end of the mass function with time. However, even if clusters acquired an infalling population following the Ilbert et al. (2010) mass function, this would not fully explain the excess of low mass galaxies observed in WINGS. The WINGS mass function at low masses is too high to be produced by the field mass function observed by Ilbert et al. (2010) (see the shape of the WINGS mass function, green long dashed line in Figure 13).

Furthermore, Bundy (2005)'s results (red filled hexagons) suggest that there are no large differences between the mass distribution of galaxies in the different environments at high-z. In this case, an environmental mass segregation + infall surely could not be responsible for the observed differences between the total mass functions in clusters at different redshifts. Unfortunately, based on these results, we are not able to securely establish whether field and cluster galaxies have similar or different mass distributions.

Focusing on the different morphological types (plots not shown), our preliminary comparison between our cluster sample and the field studies suggests that, for all types, the shape of the massive end of the mass function does not strongly depend on environment. Instead, at lower masses, there is a slight excess of field galaxies both for ellipticals and for late-types; while, the comparison of early-type galaxies (ellipticals + S0s) seems to go in the opposite direction, with clusters having proportionally more low-mass galaxies than the field.

[7] From private communication, these data are the combination of Bundy et al. (2005) and Bundy et al. (2006)

[8] The number of galaxies per unit volume in the field is of course much lower than in clusters, but here we are only interested in the shape of the distributions.

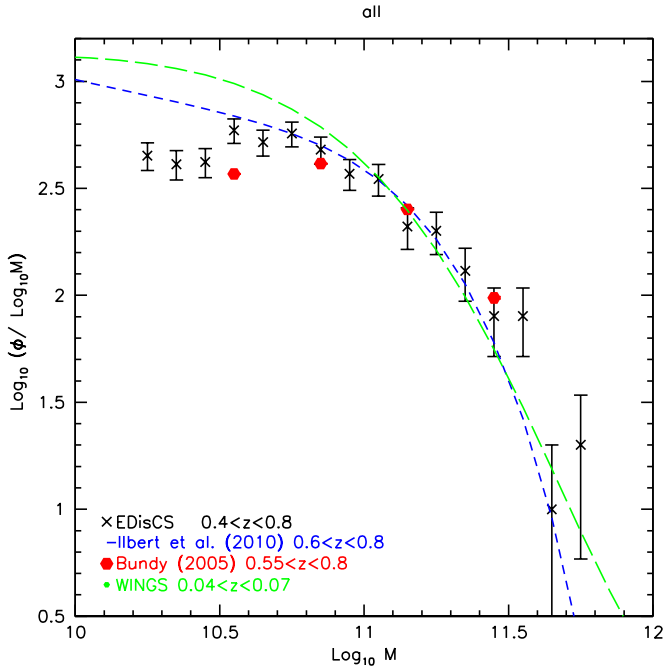

Figure 13. Comparison of the mass distribution of cluster galaxies (EDisCS - black crosses) and field galaxies (Ilbert & Bundy) at similar redshifts. Red filled hexagons are from Bundy et al. (2005) and Bundy et al. (2006). We refer briefly to them as Bundy (2005); blue dashed lines are from Ilbert et al. (2010). For comparison, we also plot the Schechter fit of the WINGS mass function (green long dashed line). Mass distributions are normalized to have the same total number of objects at $\log M_*/M_\odot \geqslant 11$. Errors are poissonian.

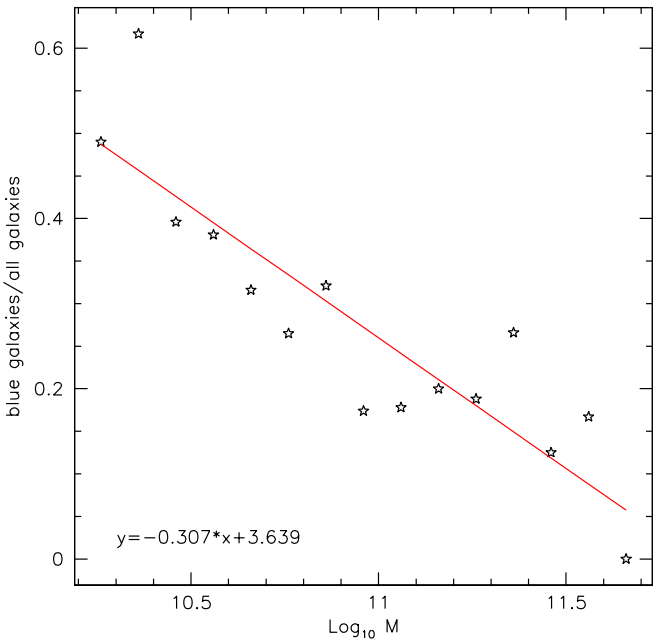

Figure 14. Fraction of blue galaxies over all galaxies as a function of the mass in the EDisCS mass limited sample. Galaxies with $(U-V)_{rest-frame} \leqslant 0.8$ are considered blue, hence star-forming. The red line represents the least squares fit performed on the points.

We have to note that these are only preliminary results, performed using heterogenous data and slightly different redshift ranges, so it cannot be used to draw definite conclusions. In the future, to establish the existence and quantify the eventual extent of an environmental mass segregation, it will be important to compare mass functions of different environments at the same redshift using homogenous data. To understand the evolution of the mass function in clusters, it will be especially useful to consider the mass function in the cluster outskirts, whose galaxies will have time to become part of clusters before $z = 0$.

Nevertheless, this preliminary comparison between the cluster and field mass functions at high-z seems to suggest that the cause for the evolution of the mass function in clusters probably needs to be sought elsewhere than in environmental mass segregation effects.

7.3 How important is star formation?

We can attempt to evaluate the importance of the contribution of star formation in changing the mass function with redshift, knowing the fraction of star-forming galaxies and the rate of mass growth due to star formation. This process doesn't act directly by changing the morphological type, but it increases the galaxy stellar mass. As previously demonstrated by several works (see e.g. Noeske et al. 2007; Feulner et al. 2005; Pérez-González et al. 2005 and our own Vulcani et al. 2010 results), low-mass galaxies have higher values of specific star formation rate (hereafter SSFR, star formation rate per unit of galaxy stellar mass) than high mass galaxies so they proportionally increase their mass much more rapidly than more massive galaxies. As a consequence, there can be some galaxies whose mass is below the mass limit at the redshift of EDisCS, but with time can grow so that they enter the sample at the redshift of WINGS, changing the shape of the mass function at low- intermediate masses.

We build a toy model to try to quantify the importance of star formation. First, we discuss an extreme case. We "simulate" a possible situation in which infall does not act and the only event is the increase of mass through star formation occurring in galaxies already located in clusters.

In clusters, star formation cannot act undisturbed from $z \sim 0.7$ to the current epoch, since there are probably several processes that cause star formation to end. Therefore, we simulate a situation in which star formation is left undisturbed only for 3 Gyr and then it stops suddenly. During the 3 Gyr, we hypothesize that it is not influenced by some external processes, so it decreases naturally with time, according to the evolution with redshift of the SSFR-Mass relation. We have chosen 3 Gyr as a "generous" timescale, as this can be considered a sort of upper limit for the time a galaxy will continue forming stars undisturbed in clusters, given the dynamical timescale in clusters ($\sim$ 1 Gyr) and the long timescale expected for some of the quenching processes proposed in clusters (e.g. strangulation, a couple of Gyrs).[9]

First of all, we take into account the fact that only star-forming galaxies grow in mass due to star formation, while passive galaxies do not. We consider as star-forming only EDisCS galaxies with $(U-V)_{rest-frame} \leqslant 0.8$ (*blue galaxies*). For each mass, we estimate the fraction of star forming galaxies, calculated as the number of

[9] Even allowing more time for the SFR to act (i.e. 6 Gyr), we found that star formation in galaxies that are already in clusters at high-z cannot be the only mechanism responsible for the observed evolution (see below).

blue galaxies over all galaxies (Figure 14). Since the relation between the fraction of blue galaxies and $\log M$ seems to be linear, we perform a least squares fit and we extrapolate the fraction also at masses below the mass completeness limit. When the fraction would turn out to be greater than 1, it is just set equal to 1.

In Vulcani et al. (2010) we analyzed the trend of the SSFR in clusters as a function of galaxy mass. We found that this trend is very similar to the trend found by Noeske et al. (2007) for the field. The main difference is that in clusters there is a population of star forming galaxies ($\sim 10\%$) that has a reduced star formation rate for their mass and that probably will end the process of star formation in the near future (for details, see Vulcani et al. 2010). So, when we consider the fraction of star forming galaxies we eliminate from the star-forming fraction 10% that corresponds to galaxies with reduced star formation.

Since we need the value of median SSFR at low masses and our cluster mass completeness limit is quite high, to estimate the mass growth we use the median SSFR-Mass relation found for the field by Noeske et al. (2007), calculated in mass bin of 0.1 dex. To reach even smaller masses, we extrapolate this relation down to $\log M_*/M_\odot \sim 8.1$ (the minimum mass of a galaxy at $z \sim 0.7$ that it turns out at $z \sim 0$ could enter our sample due to star formation). We estimate by how much galaxies can increase their mass in 3 Gyr from $z \sim 0.7$ adopting the SSFR appropriate for the epoch and the mass considered. In our estimates, we account for the fact that the observed stellar mass at any time is equal to the integral of the mass of stars formed before, minus the fraction of mass returned by stars into the interstellar phase (about 25-35% of the total mass every time the galaxy doubles its mass).

Finally, we assume that the EDisCS total mass function at masses below our mass limit remains flat, i.e. has a similar behavior to what we observe between $\log M_*/M_\odot = 10.2$ and $\log M_*/M_\odot = 10.8$. To verify this assumption where we could, we considered blue star-forming galaxies, for which we can reach a mass completeness limit lower than that of all galaxies, that is $\log M_*/M_\odot = 10.0$. Using the relation given in Figure 14, we then estimate the total number of galaxies at these low masses and we find the result to be consistent with our hypothesis that the EDisCS total mass function continues flat to low masses, at least down to $\log M_*/M_\odot = 10.0$.

According to the fractions of star forming galaxies, we add in each mass bin of the observed EDisCS total mass function, the number of galaxies that could enter that bin at $z \sim 0$, and we subtract the number of galaxies that left that bin with time. Then we normalize the new mass function so that the number of galaxies at high masses ($\log M_*/M_\odot = 11.5$, where the growth turns out to be negligible), is the same as that in the EDisCS mass function.

Figure 15 shows the results of our attempt: we find that high-z cluster members whose mass is increased due to star formation could only partially fill the observed gap between WINGS and EDisCS at low/intermediate masses. In fact, this test could fully account for the growth of the mass function only in the first bins, for $\log M_*/M_\odot \leqslant 10.4$, while the growth of intermediate masses still remains unexplained.

We stress that this result is found assuming that the high-z mass function is flat at masses below our limit, that infall is negligible and that star formation continues undisturbed for only 3 Gyr in the cluster environment.

Then, as a second more realistic test, we also take into account the contribution of infalling galaxies from the field, using Bundy et al. (2005) data. Since their data are given in mass bins of 0.3 dex, we use their same binning. As we do not know the infall rate, we cannot estimate the exact relative contribution of cluster and field galaxies. So, we normalize both the total mass function of EDisCS and that of the field to 1 and we sum them together, giving a double weight to the field galaxies. This correspond to the amount of cluster mass growth between the two redshifts from dark matter simulations (Table 4 in Poggianti et al. 2006). Then we assume that the star forming fraction at each mass is the same as that used in the previous test.[10] To extrapolate the field mass function at lower masses than the Bundy's completeness limit, we perform a Schechter fit of the field mass function. To do this, we use only Bundy's late-type galaxies since we assume that the great majority of star-forming galaxies belongs to this morphological type. Afterwards, in agreement with the previous toy model, we compute the mass growth of galaxies (both of those already in clusters and of those infallen) due to star formation in the lapse of time of 3 Gyr and estimate the new "grown" mass function.

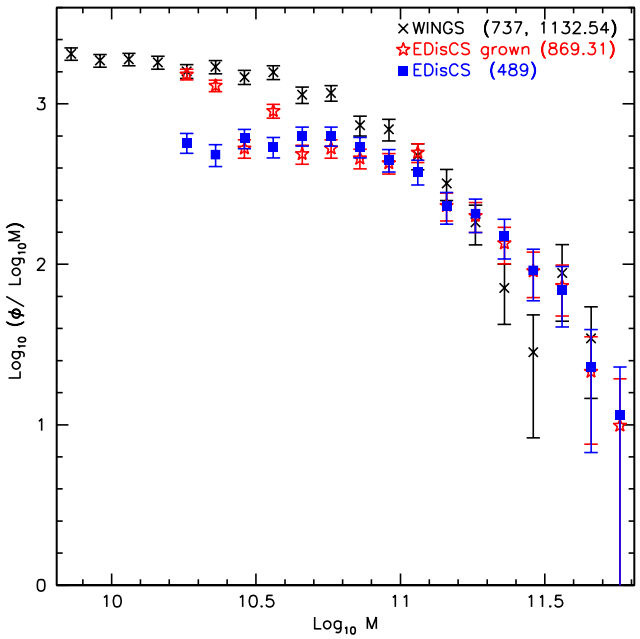

Figure 15. Comparison of the mass distribution of WINGS (black crosses) and EDisCS modified under the assumption that star formation produces an increase at intermediate masses ("EDisCS grown", red empty stars). For reference, also the EDisCS mass function is plotted (blue filled squares). WINGS and EDisCS mass functions are normalized as usual. The mass distribution of EDisCS grown is normalized to have the same total number of objects at $\log M_*/M_\odot \geqslant 11.5$ as EDisCS. Errors are poissonian. Numbers in the labels are the total number of galaxies above the respective mass completeness limit. For WINGS, both observed (first) and weighted (second) numbers are given.

Results are shown in Figure 16. Comparing the shape of the "grown" mass function, we find that it is more similar to the WINGS mass function than to the EDisCS one, from which it is derived. Our result indicates that the SFR can indeed give a non-negligible contribution to the evolution of the mass function. In this test, infalling galaxies are able to fill the gap also at intermediate masses, while this did not occur in the previous test. Impor-

[10] We can't estimate the real star forming fraction - mass relation in the field, hence we consider the relation we have found for clusters. Certainly, this is a hard lower limit and allows us to be as conservative as possible.

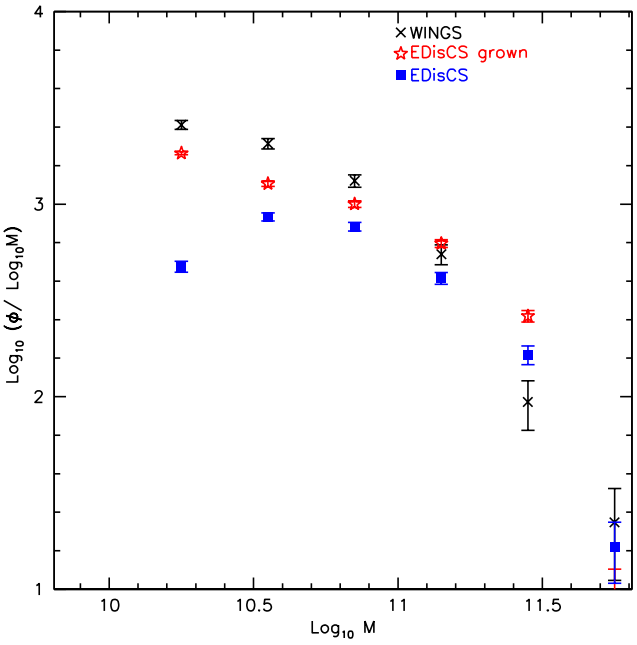

Figure 16. Comparison of the mass distribution of WINGS (black crosses) and EDisCS modified considering the contribution of the infalling galaxies and under the assumption that SF increases the mass of intermediate mass galaxies ("EDisCS grown", red empty stars). For reference, also the EDisCS mass function is reported (blue filled squares). Mass functions are normalized as usual. Errors are poissonian.

tantly, the shape of the new mass function is more similar to that of WINGS than to EDisCS.

We emphasize that in our model we have used for the field the star-forming fraction versus mass relation observed for clusters. This is surely a conservative lower limit, and therefore results in a lower limit for the contribution of infallen galaxies. We also point out that we are supposing that all field galaxies enter the clusters at $z \sim 0.7$, while galaxies enter at different epochs, and those entering later will have more time to continue forming stars and contribute to the growth of the mass function.

Moreover, we do not, for example, consider the effect of the enhanced star formation (starbursts) that might to be associated with galaxy infall into clusters (Dressler et al. 2009). This would provide an additional mass growth that helps reconcile the EDisCS and WINGS mass functions.

From these models, we suggest that star formation in both cluster galaxies and, most of all, in later infalling galaxies is probably the dominant mechanism responsible for the evolution of the total mass function. We have seen that star formation in star-forming galaxies that are already in clusters at high-z does not fully explain the observed gap in the mass functions at the two redshifts, while adding the infalling field population more closely reproduces the observed mass function at low-z.

This shows that infall does play a role, contributing a large number of low mass galaxies that, as long as they continue forming stars, increase their mass due to star formation. In §7.2 we have seen that it is currently unclear whether, in addition to this effect, infall also contributes to the evolution of the mass function via environmental mass segregation, by directly increasing the relative numbers of low-mass ($\log M_*/M_\odot = 10.2-10.8$) versus high-mass galaxies $\log M_*/M_\odot \geqslant 10.8$.

In our test we have conservatively adopted the mass function of Bundy et al. (2005) that, as we have seen in §7.2, is more similar to the EDisCS mass function and suggests no environmental mass segregation. If the field mass function was steeper at lower masses (as Ilbert et al. (2010) find), the contribution of the mass growth due to star formation in infalling galaxies could be even stronger.

Obviously, star formation can affect the evolution of the late-type galaxy and total mass functions, but alone cannot explain the observed evolution of the mass function of early-type galaxies. Moreover, star formation cannot be directly responsible for the observed evolution in the morphological mix. Some other mechanism/s must be at work transforming late-type galaxies into early-types, thereby changing the shape of the early-type mass functions.[11]

8 SUMMARY AND CONCLUSIONS

In this paper, we have characterized the stellar mass functions and their evolution from $z = 0.8$ to $z = 0$ of two mass limited samples of galaxies in clusters drawn from the WINGS ($\log M_*/M_\odot > 9.8$) and EDisCS ($\log M_*/M_\odot > 10.2$) datasets. We considered both the total mass function and the mass function of different morphological types. We then analyzed the morphological fractions both for mass limited and magnitude limited samples.

Our main results are:

- The total stellar mass distribution of galaxies in clusters evolves with redshift. In a mass-limited sample, clusters at high-z have on average more massive galaxies than at low-z. Assuming no evolution at the massive end, the population of $10.2 \geqslant \log M_*/M_\odot \leqslant 10.8$ galaxies must have grown significantly between $z = 0.8$ and $z = 0$.
- At low redshift, different morphological types have significantly different mass functions, although S0s and late-type galaxies more massive than $\log M_*/M_\odot = 10.2$ may have similar mass distributions. At high redshift our results are not conclusive.
- The mass distribution of *each* morphological type evolves with redshift. In all types there are proportionally more massive galaxies at high- than at low-z.
- Both for the mass-limited and the magnitude-limited samples, the proportion of galaxies of different morphological types as a function of galaxy stellar mass (the morphology-mass relation) evolves strongly with redshift, as expected given the evolution of the morphological fractions. At both redshifts, in the mass limited sample, the incidence of each type does not strongly depend on mass up to $\log M_*/M_\odot \sim 11$. Above this value, ellipticals dominate.
- Both considering a mass limited and a magnitude limited sample, and in agreement with previous magnitude-limited works (e.g. Dressler et al. 1997; Fasano et al. 2000; Postman et al. 2005; Smith et al. 2005; Desai et al. 2007; Poggianti et al. 2009), we find that the number fraction of elliptical galaxies is almost constant

[11] We note that such mechanism can in principle be itself mass-dependent, and could transform low-mass galaxies more efficiently than high-mass galaxies. In this scenario, also harassment, by stripping mass to galaxies and making them change their morphology, could partly contribute to the change of the mass functions type by type.

with redshift ($\sim$ 30%). In contrast, the fraction of S0s and late-types considerably changes with time (S0s $\sim$ 50% at the current epoch, late-type $\sim$ 55% in the distant Universe), as also reported in those other studies.

- In addition to the number fraction of ellipticals, also the fraction of stellar mass in ellipticals remains constant with redshift, being about 40% both in EDisCS and in WINGS. At high-z, 13% of the stellar mass is in S0s, and 46% in later types. At low-z, the mass fractions are inverted: 42% in S0s, and 15% in late-types.

The most likely explanation of the observed evolution of the mass functions is the mass growth of galaxies due to star formation in both cluster galaxies and, most of all, in galaxies infalling from the cluster surrounding areas. In this way, galaxies that are not part of our distant universe sample, after a reasonable lapse of time, can increase their mass due to star formation so that they can enter our local Universe sample.

Therefore, infall does play a role contributing a large number of star-forming galaxies growing their mass. In principle, infall could also contribute by directly increasing the population of low-mass galaxies compared to the massive population, due to infalling galaxies having a different mass distribution from galaxies already in clusters at high-z. However, we do not find conclusive evidence for such environmental mass segregation in our comparison with field studies.

In the future, it will be important to compare the galaxy stellar mass distribution in cluster cores, cluster infalling regions, groups and the field using homogeneous data, to conclusively establish whether and how much the total galaxy stellar mass function depends on environment at different redshifts.

Finally, star formation, acting mainly on late-type galaxies, can directly affect the evolution of the total and late-type galaxy mass functions, however it cannot directly account for the observed evolution of early-type galaxies. Subsequent morphological transformations from late to early types likely cause the evolution of the mass functions of S0s and ellipticals.

ACKNOWLEDGMENTS

We thank Alessandro Bressan for providing IMF conversion factors; Kevin Bundy for providing us his data and support. We thank John Moustakas and Patricia Sánchez-Blázquez for providing us their estimation of stellar masses and for helpful discussions. We thank Vandana Desai for performing the visual classification of WINGS galaxies. We thank Kai Noeske and the AEGIS collaboration for providing us their data. We thank the anonymous referee, whose comments helped us to improve the quality of this work. BV and BMP acknowledge financial support from ASI contract I/016/07/0.

APPENDIX A: THE RELIABILITY OF EDISCS PHOTO-Z MASS FUNCTIONS

Throughout the paper, for EDisCS, we have used the photo-z membership. Here we show that, in the mass range in common, the mass function determined from photo-z's is in agreement within the errors with the mass function determined using only spectroscopic members and spectroscopic completeness weights, derived similarly to what we have done for WINGS. The two mass functions for the mass limited sample are shown in (Figure A1). In this comparison, we are using all photo-z and spectroscopic members, without considering their R_{200} or their morphology.

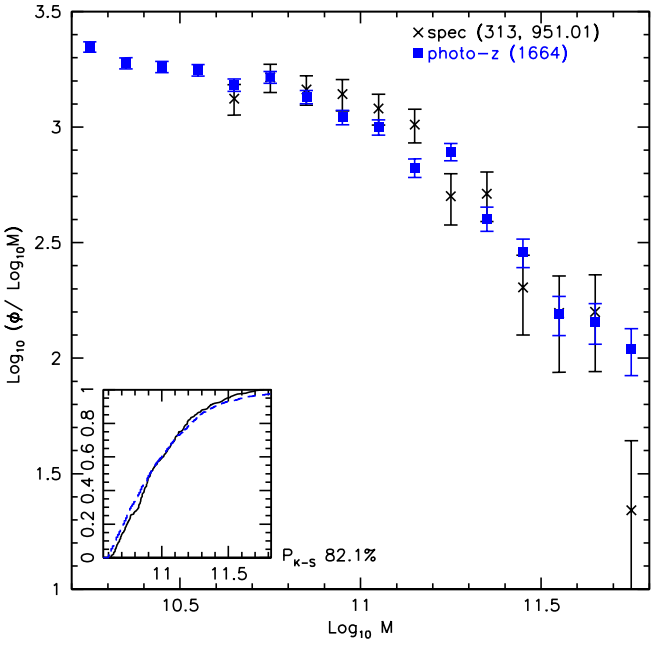

Figure A1. Comparison between the mass distribution of all EDisCS galaxies with spectroscopic membership (black crosses) and photo-z membership (blue filled squares). Mass distributions are normalized to have the same total number of objects at $\log M_*/M_\odot \geqslant 11$. Errors are poissonian. In the insets the cumulative distributions above the same mass limit are shown.

A K-S test above $\log M_*/M_\odot = 10.6$ cannot reject the hypothesis that the two samples are drawn from the same parent distribution (K-S probability $\sim$ 82.1%). This gives us confidence in using the photo-z's, that allow us to reach much deeper mass limits.

APPENDIX B: THE MAGNITUDE COMPLETENESS LIMIT

In this Appendix we show the mass distributions in magnitude limited samples, considering the same magnitude limits adopted by the morphological fraction studies (§6.1). We show how this choice alters the final results: in fact, these mass distributions are very different from those we derive using mass limited samples.

In mass selected samples only a modest and systematic evolution of galaxy masses with time is expected, unlike magnitude selected samples where galaxies can enter and leave the sample due to variations in their star formation activity. A mass selection gives a more robust mean of identifying likely progenitors of z=0 cluster galaxies in higher redshift clusters. However, we note that also in mass limited samples some progenitors could lack. First, galaxies can continue to grow in mass and so some galaxies that weren't included at high redshift enter in the sample at low redshift, moreover the infall of galaxies from the field can alter the mass distribution.

It is important to note that the choice of a magnitude limit implies a natural mass limit below which the sample is incomplete. This corresponds to the mass of the reddest galaxy at the limiting magnitude.

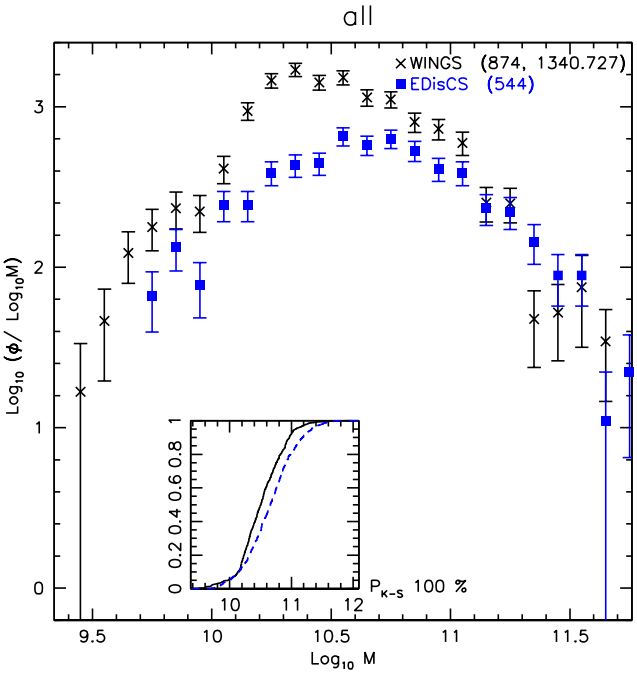

Figure B1. Comparison of the mass distribution of EDisCS (blue filled squares) and WINGS (black crosses) galaxies, of all morphological types, for the magnitude limited samples. Mass distributions are normalized to have the same total number of objects at $\log M_*/M_\odot \geqslant 11$. Errors are poissonian. In the insets the cumulative distributions are shown.

For WINGS, $M_V = -19.5$, and $B-V = 1.2$, the mass completeness limit corresponds to a $M \sim 10^{10.5} M_\odot$.

For EDisCS, $M_V = -20$, and $B-V = 0.9$, it corresponds to a $M \sim 10^{10.4} M_\odot$.

When using magnitude limited samples, it should therefore always be kept in mind that below the mass completeness limit the sample is incomplete, hence results will differ from those obtained from a complete (e.g. mass limited) sample. In the following, we show some examples. These plots have to be directly compared with those already presented in this paper.

Figure B1 shows the mass distribution of all galaxies, regardless of their morphological type, for WINGS and EDisCS galaxies in the magnitude limited sample. Both distributions rise, reach a peak, then decline again.

For WINGS, for which the completeness mass limit of the magnitude limited sample is much higher than the limit of the mass limited sample, it is clear that the shape of the distribution below the completeness mass limit is very different from the one obtained for the mass limited sample (cfr. Figure B1 with Fig. 3). Instead, no significant change is expected nor observed between the mass limited and the magnitude limited distributions above $\log M_*/M_\odot \sim 10.5$.

As for the mass limited samples, the mass functions of WINGS and EDisCS are very different. If we consider the whole mass range covered by galaxies in the magnitude limited sample, a K-S test rejects the null hypothesis of similar mass distribution with a probability 100%.

Then, we also show (Figure B2) the comparison of the mass distribution of the different morphological types at the two redshifts, to be contrasted with the mass-limited ones in Fig. 5. Again, in the magnitude limited samples, incompleteness setting in below the completeness mass limit creates a spurious declining trend at low masses.

The comparison of magnitude-limited and mass-limited samples clearly shows that the mass distribution derived from the former is meaningless, because affected by incompleteness, below the the limit corresponding to the mass of a galaxy with the reddest color and the faintest magnitude in the sample.

REFERENCES

Andreon, S. 2006, AAp, 448, 447
Aragon-Salamanca, A., et al. 1993, MNRAS, 262, 764
Aragón-Salamanca, A. et al. in preparation
Baldry, I. K., et al. 2004, ApJ, 600, 681
Baldry, I. K., et al. 2006, MNRAS, 373, 469
Baldry, I. K., et al. 2008, MNRAS, 388, 945
Balogh, M. L., et al. 2001, ApJ, 557, 117
Barger, A. J., et al. 1998, ApJ, 501, 522
Bell, E. F., & de Jong, R. S. 2001, ApJ, 550, 212
Bell, E.F., et al., 2007, ApJ, 663, 834
Bekki, K. 1998, ApJL, 502, L133
Bekki, K. 2009, MNRAS, 399, 2221
Blanton, M. R., & Roweis, S. 2007, AJ, 133, 734
Bolzonella, M., et al. 2000, AAp, 363, 476
Bolzonella, M., et al. 2009, arXiv:0907.0013
Borch, A., et al. 2006, AAp, 453, 869
Boselli, A., & Gavazzi, G. 2006, PASP, 118, 517
Brinchmann, J., et al. 2004, MNRAS, 351, 1151
Brunner, R. J., & Lubin, L. M. 2000, AJ, 120, 2851
Bundy, K.,et al. 2005, ApJ, 625, 621
Bundy, K., et al. 2006, ApJ, 651, 120
Byrd, G., & Valtonen, M. 1990, ApJ, 350, 89
Capak, P., et al. 2007, ApJS, 172, 284
Cava, A., et al. 2009, AAp, 495, 707
Conselice, C. J., et al. 2000, ApJ, 529, 886
Conselice, C. J. 2003, ApJS, 147, 1
De Propris, R., et al. 2007AJ, 133, 2209
Desai, V., et al. 2007, ApJ, 660, 1151
Dressler, A. 1980, ApJ, 236, 351
Dressler, A., et al. 2009, ApJ, 693, 140
Dressler, A., et al. 1997, ApJ, 490, 577
Drory, N., et al. 2005, ApJL, 619, L131
Ebeling, H., et al. 1996, MNRAS, 281, 799
Ebeling, H., et al. 1998, MNRAS, 301, 881
Ebeling, H., et al. 2000, MNRAS, 318, 333
Ellison, S. L., et al. 2010, arXiv:1002.4418
Fasano, G., et al. 2000, ApJ, 542, 673
Fasano, G., et al. 2006, AAp, 445, 805
Fasano, G., et al. 2007, From Stars to Galaxies: Building the Pieces to Build Up the Universe, A. Vallenari, R. Tantalo, L. Portinari, & A. Moretti, ASP Conference Series, 374, 495
Fasano, G., et al. 2010, MNRAS, 404, 1490
Fasano, G., et al. 2010, in preparation
Feulner, et al. 2005, ApJL, 633, L9
Finn, R. A., et al. 2005, ApJ, 630, 206
Finn, R. A., et al. 2010, ApJ, submitted
Font, A. S.,et al. 2008, MNRAS, 389, 1619
Fontana, A., et al. 2004, AAp, 424, 23
Fontana, A., et al. 2006, AAp, 459, 745
Franceschini, A., et al. 2006, AAp, 453, 397
Fritz, J., et al.2007, AAp, 470, 137

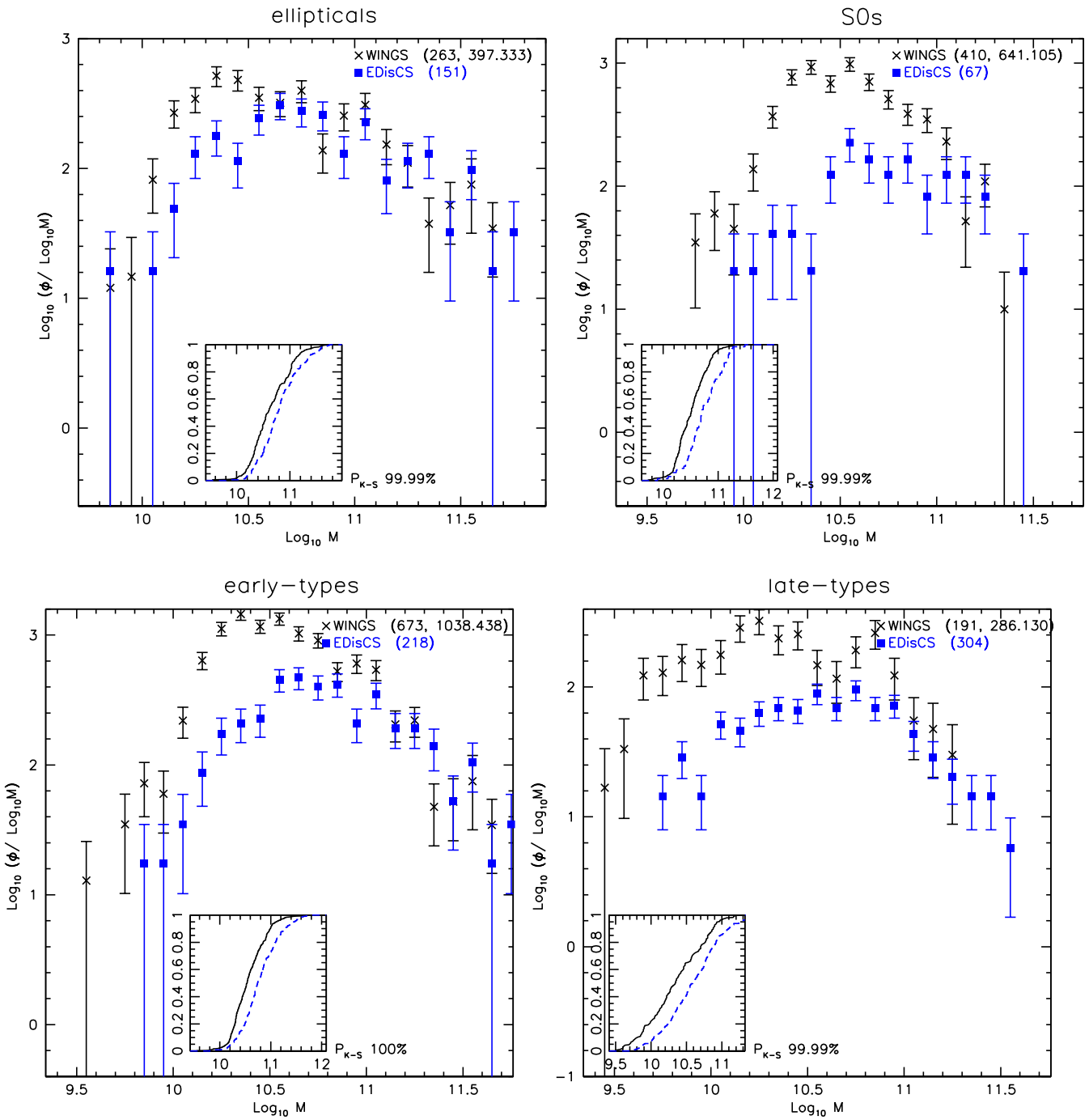

Figure B2. Comparison of the mass distribution of EDisCS (blue open circles) and WINGS (red stars) galaxies, for different morphological types, in magnitude limited samples. Mass distributions are normalized to the total number of objects with $\log M_*/M_\odot \geqslant 11$. In the insets the cumulative distributions are shown.

Fritz, J., et al. 2010, in preparation
Gehrels, N. 1986, ApJ, 303, 336
Gonzalez, A. H., et al. 2001, ApJS, 137, 117
Gunn, J. E., & Gott, J. R., III 1972, ApJ, 176, 1
Gwyn, S. D. J., & Hartwick, F. D. A. 2005, AJ, 130, 1337
Halliday, C., et al. 2004, AAp, 427, 397
Holden, B. P., et al. 2007, ApJ, 670, 190
Huertas-Company, et al. 2009, AAp, 505, 83
Icke, V. 1985, AAp, 144, 115
Ilbert, O., et al. 2010, ApJ, 709, 644
Kauffmann, G. 1995, MNRAS, 274, 161
Kauffmann, G.,et al. 2003, MNRAS, 341, 54
Kodama, T., & Bower, R. 2003, MNRAS, 346, 1
Kovac, K., et al. 2009, arXiv:0909.2032
Kroupa, P. 2001, MNRAS, 322, 231
Larson, R. B., et al. 1980, ApJ, 237, 692
Lotz, J. M., Primack, J., & Madau, P. 2004, AJ, 128, 163
Makino, J., & Hut, P. 1997, ApJ, 481, 83

McCarthy, I. G., et al. 2008, MNRAS, 383, 593
Milvang-Jensen, B., et al. 2008, AAp, 482, 419
Mihos, J. C. 2004, Clusters of Galaxies: Probes of Cosmological Structure and Galaxy Evolution, 277
Moore, B., et al. 1996, Nature, 379, 613
Noeske, K. G., et al. 2007, ApJL, 660, L47
Ocvirk, P., et al. 2006, MNRAS, 365, 74
Ocvirk, P. 2010, ApJ, 709, 88
Oesch, P. A., et al. 2010, ApJL, 714, L47
Omizzolo, A 2010 in preparation
Ostriker, J. P. 1980, Comments on Astrophysics, 8, 177
Pannella, M., et al. 2006, ApJL, 639, L1
Pelló, R., et al. 2009, AAp, 508, 1173
Pérez-González, P. G., et al. 2005, ApJ, 630, 82
Poggianti, B. M. 1997, AApS, 122, 399
Poggianti, B. M., et al. 2006, ApJ, 642, 188
Poggianti, B. M., et al. 2008, ApJ, 684, 888
Poggianti, B. M., et al. 2009, ApJL, 697, L137
Postman, M., et al. 2005, ApJ, 623, 721
Pozzetti, L., et al. 2007, AAp, 474, 443
Pozzetti, L., et al. 2009, arXiv:0907.5416
Rudnick, G., et al. 2001, AJ, 122, 2205
Rudnick, G., et al. 2003, ApJ, 599, 847
Rudnick, G., et al. 2009, ApJ, 700, 1559
Salpeter, E. E. 1955, ApJ, 121, 161
Sánchez-Blázquez, P., et al. 2006, MNRAS, 371, 703
Schechter, P. 1976, ApJ, 203, 297
Smith, G. P., et al. 2005, ApJ, 620, 78
Tasca, L. A. M., et al. 2009, AAp, 503, 379
Toft, S., et al. 2004, AAp, 422, 29
Valentinuzzi, T., et al. 2009, AAp, 501, 851
Valentinuzzi, T., et al. 2010, ApJ, 712, 226
Varela, J., et al. 2009, AAp, 497, 667
van der Wel, A., et al. 2007, ApJ, 670, 206
van der Wel, A. 2008, ApJL, 675, L13
Vazdekis, A. 2009, American Institute of Physics Conference Series, 1111, 39
Vergani, D., et al. 2008, AAp, 487, 89
von der Linden, et al. 2010, MNRAS, 404, 1231
Vulcani, B., et al. 2010, ApJL, 710, L1
White, S. D. M., et al. 2005, AAp, 444, 365